Dark matter searches with cosmic antideuterons and antihelium

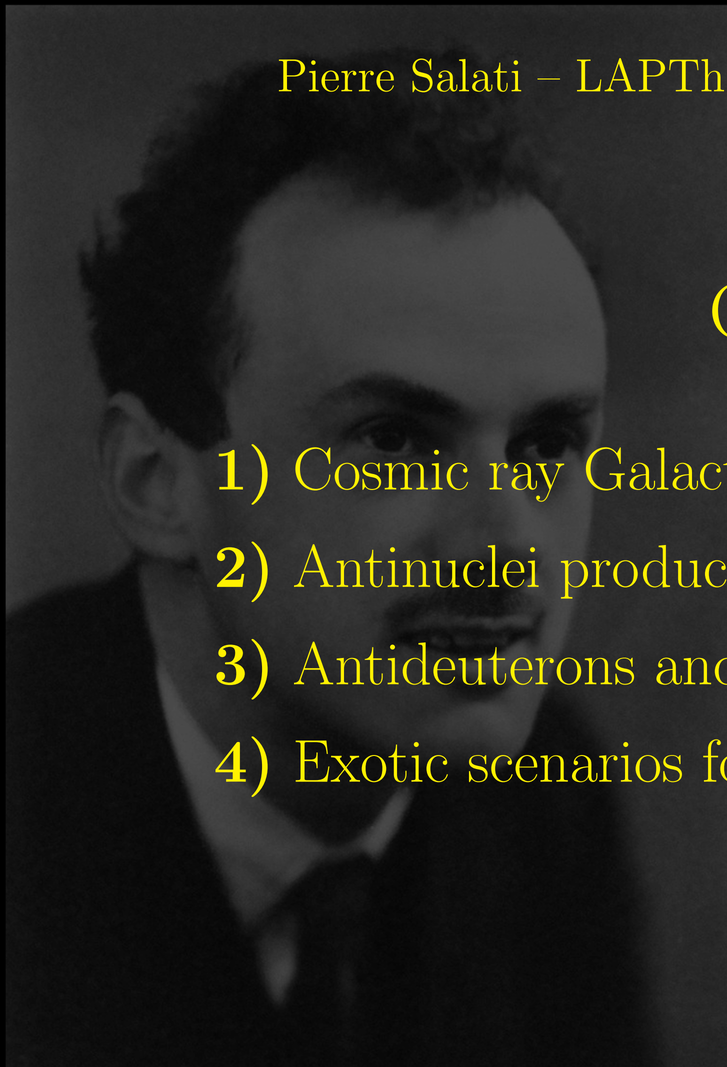

Pierre Salati – LAPTh & Université Savoie Mont Blanc

Outline

1) Cosmic ray Galactic propagation

2) Antinuclei production through coalescence

3) Antideuterons and the canonical approach

4) Exotic scenarios for antihelium DM production

JENAA workshop on Nuclear Physics at the LHC and connections to astrophysics – August 19, 2024

The putative AMS-02 antihelium events

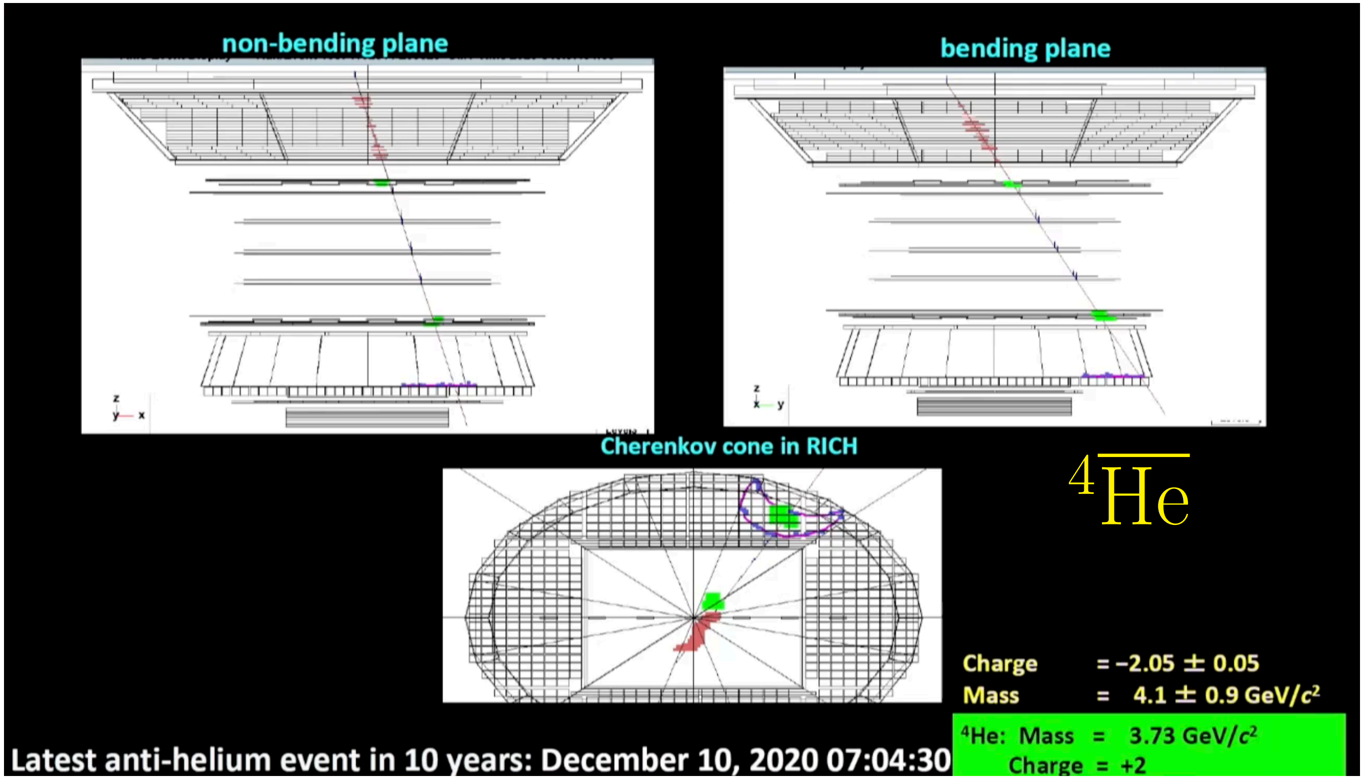

V. Choutko, Cosmic Heavy Anti-Matter, COSPAR E1.3-05-22, July 17th 2022

- AMS-02 has observed few events in the mass region from 0 to 10 GeV with charge $Z = -2$ and rigidity $\mathcal{R} < 50\,\mathrm{GV}$. The masses of all events are in the $^3\overline{\mathrm{He}}$ and $^4\overline{\mathrm{He}}$ mass region. As of 2018, 6 events $^3\overline{\mathrm{He}}$ and 2 events $^4\overline{\mathrm{He}}$.

- The event rate is $\sim$ 1 antihelium in 100 million helium.

- Massive MC background simulations are carried out to evaluate significance. So far 35 billion He events simulated vs 6.8 billion He event triggers for 10 years. AMS-02 did not find background to the antihelium events. At this level, the MC simulations are difficult to validate.

1) Cosmic ray Galactic propagation

$$q_{\rm sec}(\bar{\rm A}\,|\,E_{\bar{\rm A}},\boldsymbol{x}) = \sum_{i\in {\rm p},\alpha}\;\sum_{j\in {\rm H,He}} 4\,\pi \int dE_i\;\Phi_i(E_i,\boldsymbol{x})\,n_j(\boldsymbol{x})\,\frac{d\sigma_{ij\to\bar{\rm A}}}{dE_{\bar{\rm A}}}(E_i,E_{\bar{\rm A}})$$

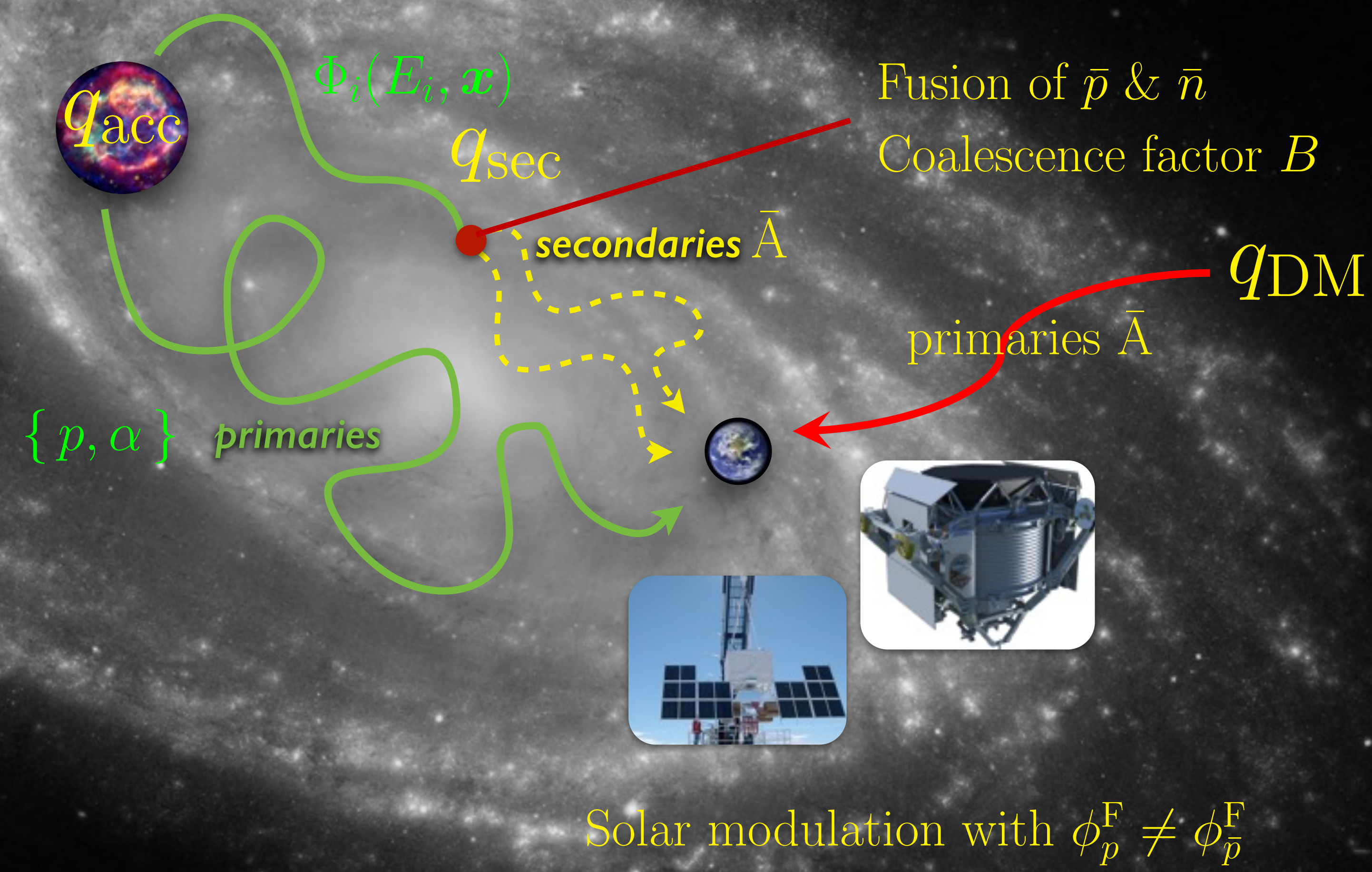

Courtesy Antje Putze, TeVPA 2015

1) Cosmic ray Galactic propagation

$$q_{\rm DM}(\bar{\rm A}\,|\,E_{\bar{\rm A}},\boldsymbol{x}) = \frac{1}{2}\left\{\frac{\rho_{\rm DM}(\boldsymbol{x})}{m_{\rm DM}}\right\}^2 \sum_{\rm channel\,F} \langle\sigma_{\rm ann}v\rangle_{\rm F} \times \frac{d\mathcal{N}^{\rm F}_{\bar{\rm A}}}{dE_{\bar{\rm A}}}$$

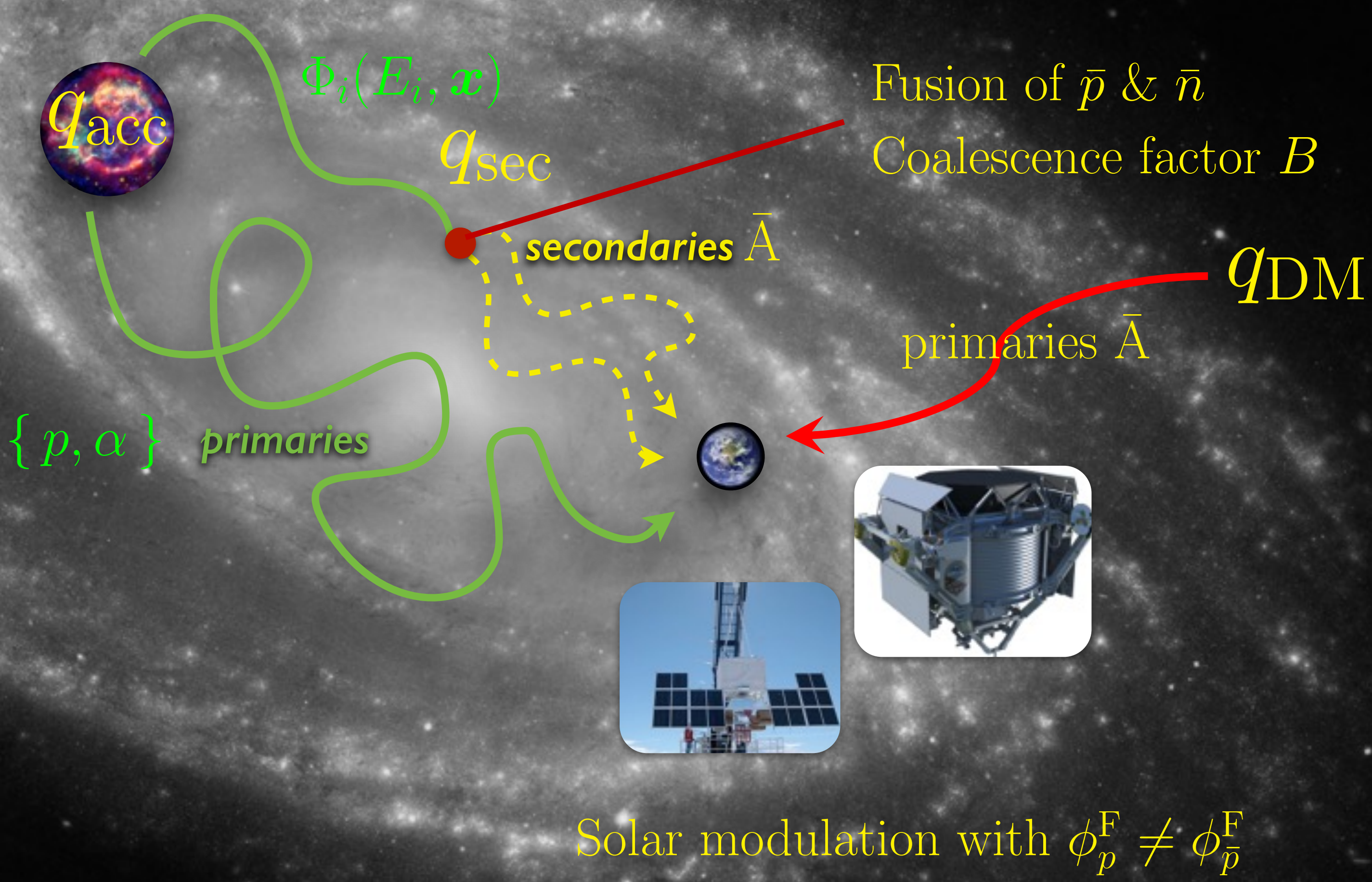

Courtesy Antje Putze, TeVPA 2015

1) Cosmic ray Galactic propagation

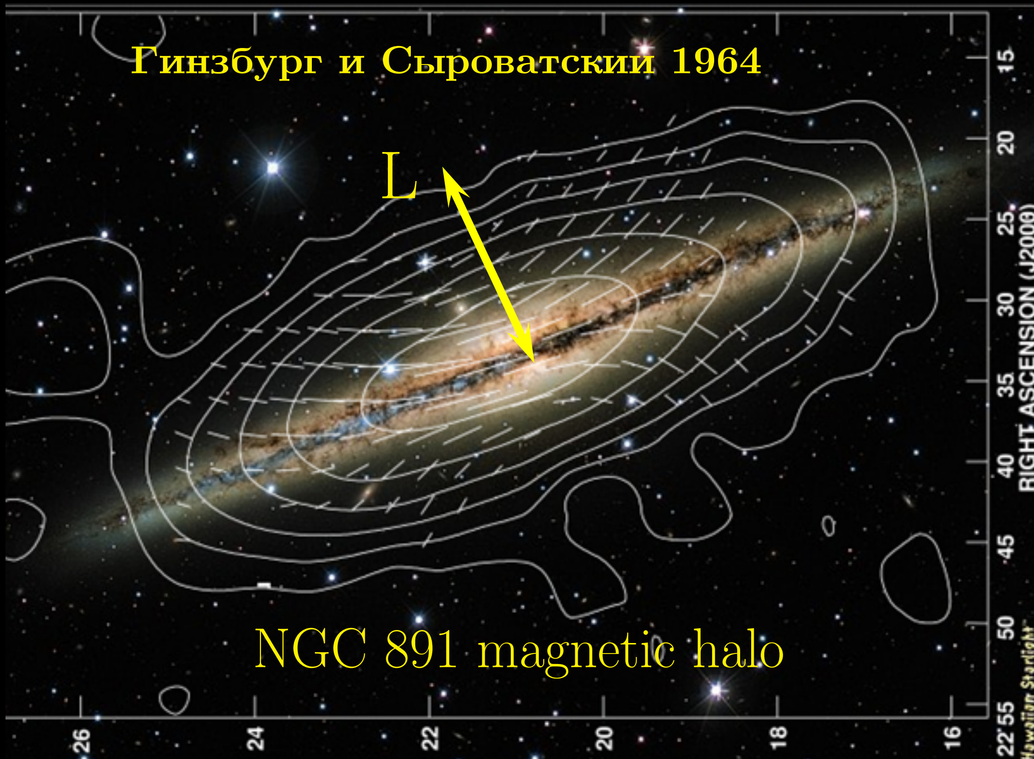

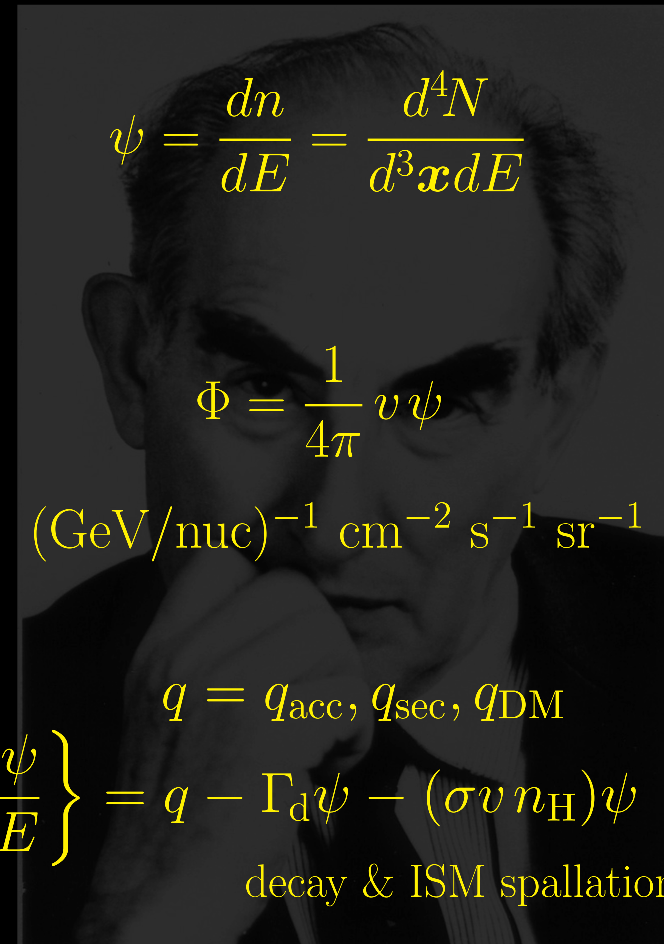

$$\psi = \frac{dn}{dE} = \frac{d^4 N}{d^3 \boldsymbol{x}\, dE}$$

$$\Phi = \frac{1}{4\pi} v \psi$$

$(\mathrm{GeV/nuc})^{-1}\ \mathrm{cm}^{-2}\ \mathrm{s}^{-1}\ \mathrm{sr}^{-1}$

$$q = q_{\rm acc}, q_{\rm sec}, q_{\rm DM}$$

$$\dot{\psi} + \boldsymbol{\nabla}\cdot\{-K\,\boldsymbol{\nabla}\psi + \psi \boldsymbol{V}_C\} + \frac{\partial}{\partial E}\left\{b\,\psi - D_{EE}\frac{\partial \psi}{\partial E}\right\} = q - \Gamma_{\rm d}\psi - (\sigma v\, n_{\rm H})\psi$$

convection

E losses

decay & ISM spallation

$\boldsymbol{x}$ diffusion

E diffusion

$$K = \beta^{\eta} K_0 \left\{1 + \left(\frac{R_{\rm l}}{R}\right)^{\frac{\delta-\delta_{\rm l}}{s_{\rm l}}}\right\}^{s_{\rm l}} \left(\frac{R}{1\,\mathrm{GV}}\right)^{\delta} \left\{1 + \left(\frac{R}{R_{\rm h}}\right)^{\frac{\delta-\delta_{\rm h}}{s_{\rm h}}}\right\}^{-s_{\rm h}}$$

$$D_{EE} = \frac{4}{3}\frac{\beta^2}{\delta(4-\delta^2)(4-\delta)}\frac{{V_a}^2 p^2}{K}$$

1) Cosmic ray Galactic propagation

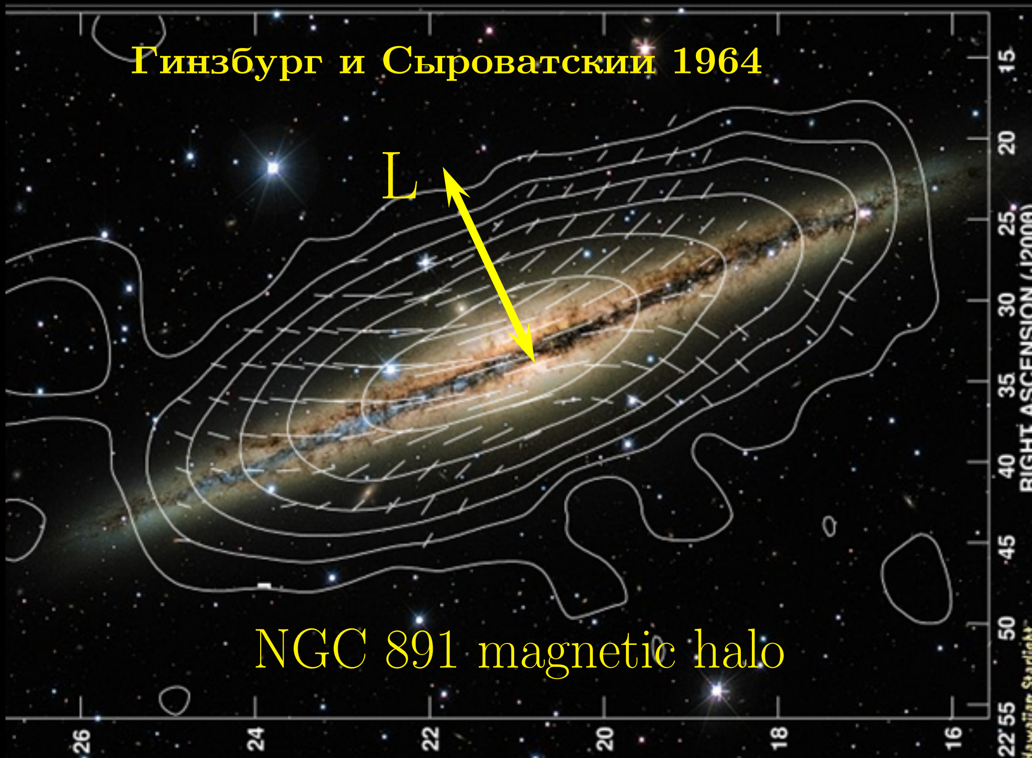

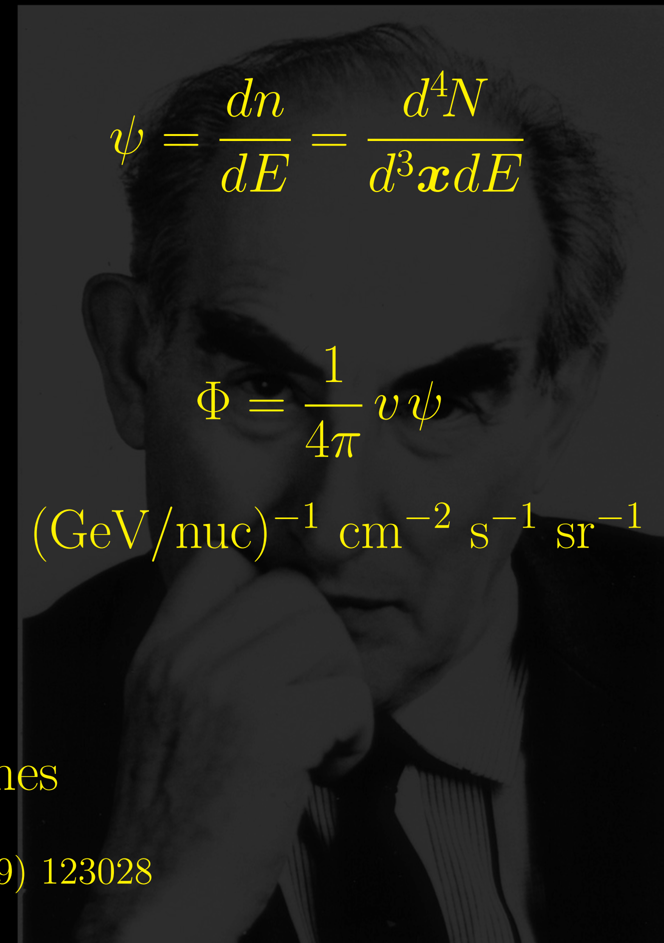

$$\psi = \frac{dn}{dE} = \frac{d^4N}{d^3\boldsymbol{x}\,dE}$$

$$\Phi = \frac{1}{4\pi} v\psi$$

$(\mathrm{GeV/nuc})^{-1}\ \mathrm{cm}^{-2}\ \mathrm{s}^{-1}\ \mathrm{sr}^{-1}$

Three CR transport schemes

Y. Génolini et al., Phys. Rev. **D99** (2019) 123028

- BIG is the most comprehensive (K_0, δ, R_l, δ_l, V_C, V_a, L)
- QUAINT $\subset$ BIG is the old scheme (K_0, δ, η, V_C, V_a, L)
- SLIM $\subset$ BIG is for the Gifted Amateur (K_0, δ, R_l, δ_l, L)

1) Cosmic ray Galactic propagation

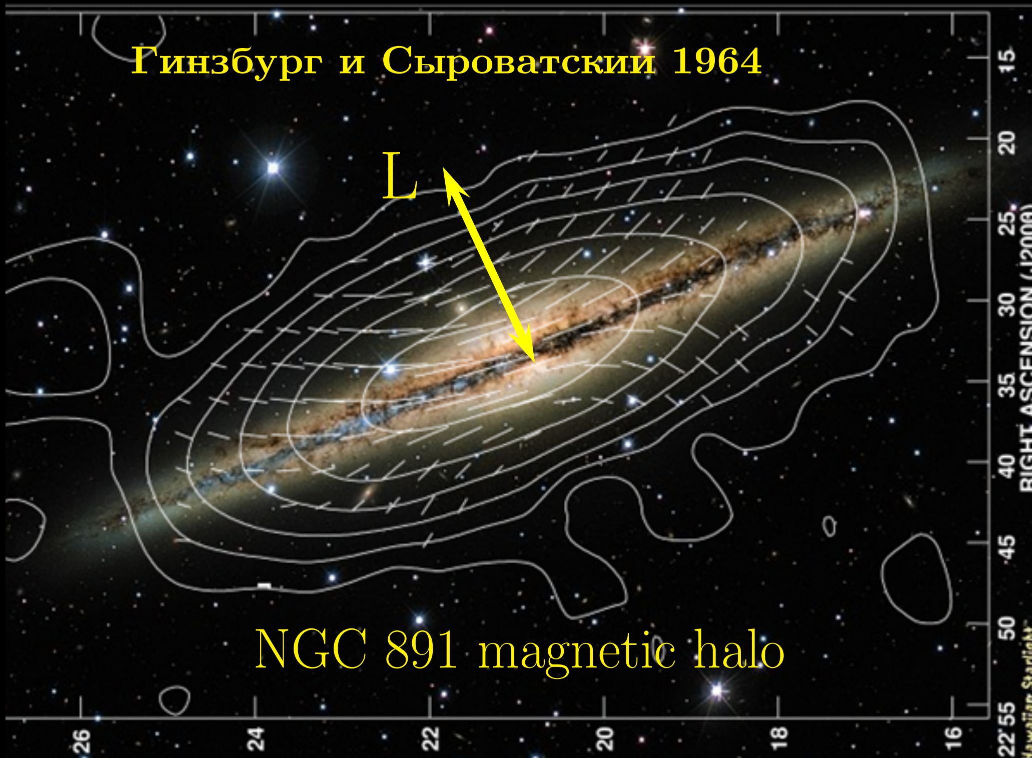

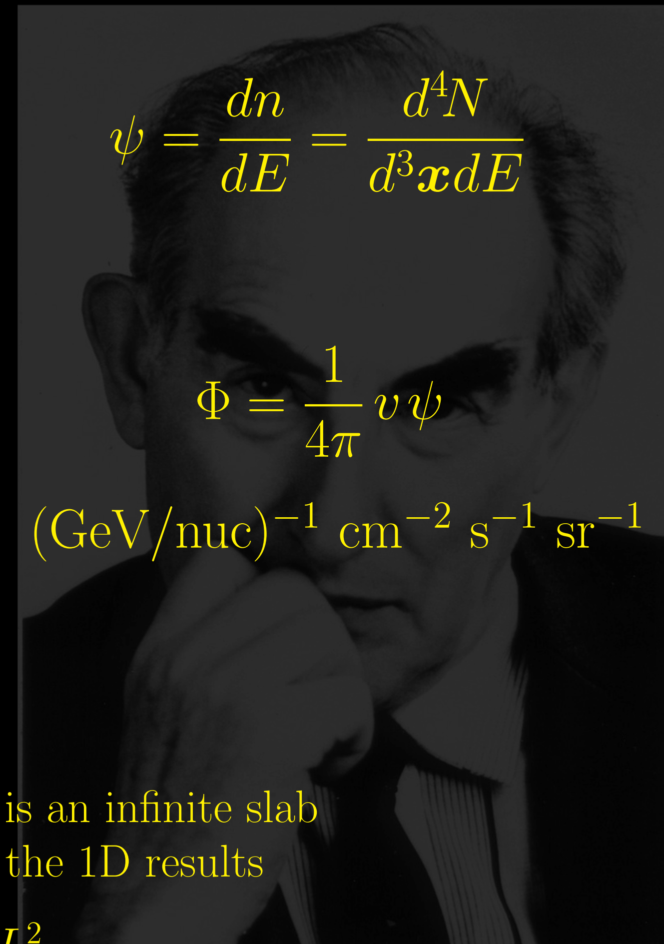

$$\psi = \frac{dn}{dE} = \frac{d^4N}{d^3\boldsymbol{x}\,dE}$$

$$\Phi = \frac{1}{4\pi} v \psi$$

$$(\mathrm{GeV/nuc})^{-1}\ \mathrm{cm}^{-2}\ \mathrm{s}^{-1}\ \mathrm{sr}^{-1}$$

Assuming that the Milky Way magnetic halo is an infinite slab and that diffusion alone is at work, we get the 1D results

$$\psi_{\mathrm{sec}} = \frac{hL}{K} \times q_{\mathrm{sec}} \quad \text{while} \quad \psi_{\mathrm{prim}} = \frac{L^2}{2K} \times q_{\mathrm{DM}}$$

B/C analyses fix the ratio L/K

L is required to get the flux of antinuclei from DM

1) Cosmic ray Galactic propagation

- ^{10}**Be** used as a CR clock with half-lifetime $t_{1/2}$ of 1.387 Myr
- But isotopic data at low energies and with improvable precision
- Trade-off between isotopic data ^{10}**Be/Be** & ^{10}**Be/^{9}Be** and elemental ratio **Be/B**

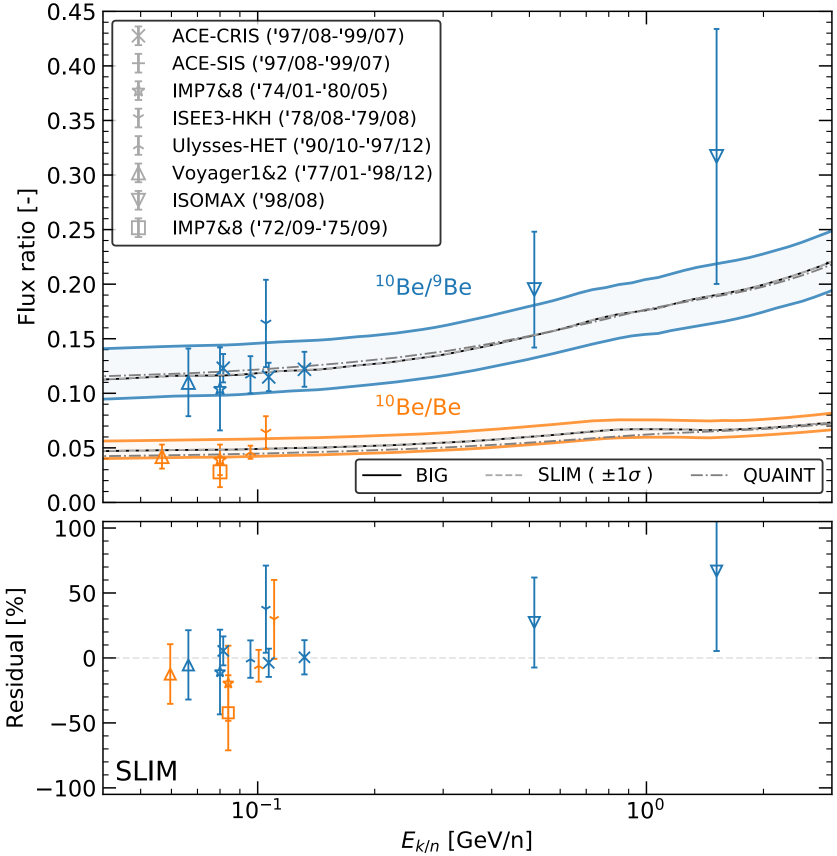

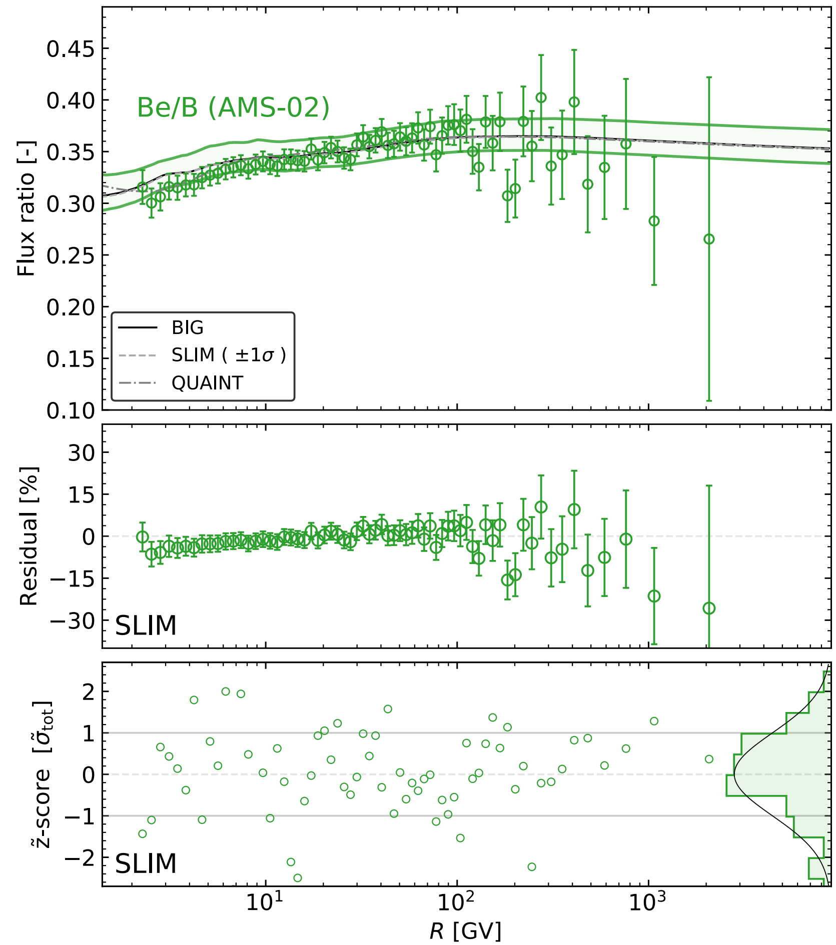

Weinrich+[2002.11406] & Weinrich+2004.00441]

1) Cosmic ray Galactic propagation

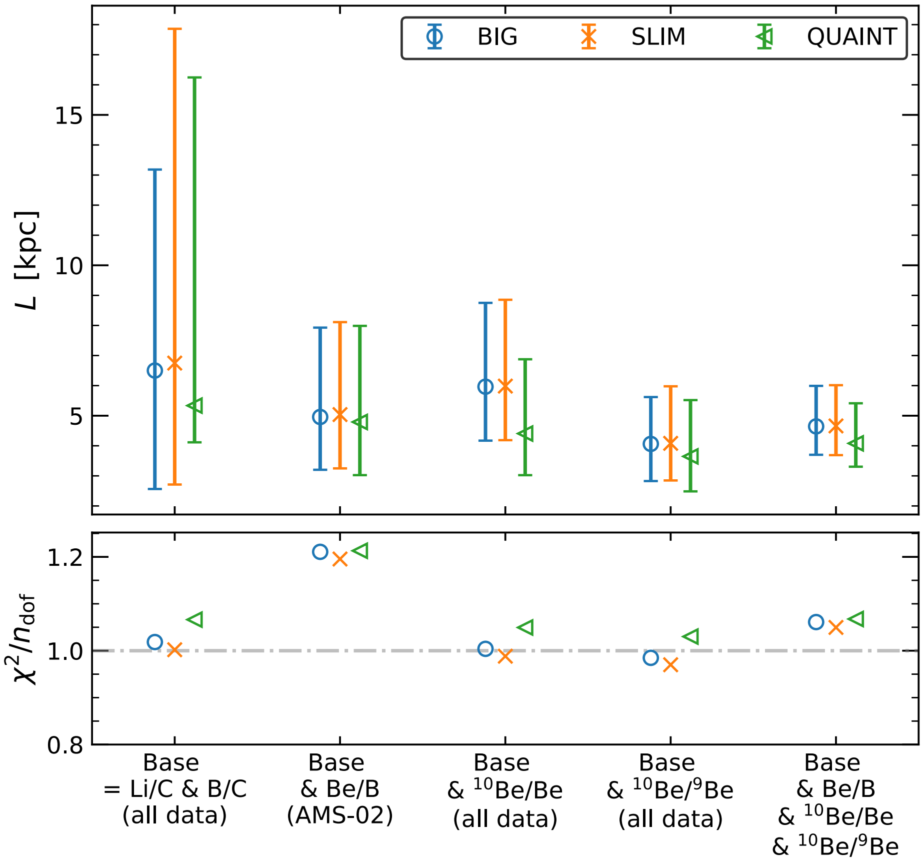

	BIG	SLIM	QUAINT
	Base & Be/B (AMS-02)		
L [kpc]	$4.96^{+2.97}_{-1.76}$	$5.04^{+3.07}_{-1.79}$	$4.79^{+3.19}_{-1.77}$
$\chi^2 / n_{\rm dof}$	233.7 / 193	233.1 / 195	235.3 / 194
$\chi^2_{\rm nui} / n_{\rm nui}$	17.4 / 20	17.4 / 20	15.8 / 20
	Base & Be/B & ^{10}Be/Be & ^{10}Be/^{9}Be (all data)		
L [kpc]	$4.64^{+1.35}_{-0.94}$	$4.66^{+1.35}_{-0.97}$	$4.08^{+1.33}_{-0.78}$
$\chi^2 / n_{\rm dof}$	266.3 / 251	265.6 / 253	269.0 / 252
$\chi^2_{\rm nui} / n_{\rm nui}$	25.6 / 35	25.4 / 35	25.6 / 35

$\log_{10} L$	δ	$\log_{10} K_0$	V_A	R_l	δ_l	V_c
0.667	0.498	−1.446	5.000	4.493	−1.102	0.140

$$\begin{pmatrix}
+4.20\text{e-}3 & +3.53\text{e-}4 & +3.94\text{e-}3 & +1.49\text{e-}2 & +2.57\text{e-}3 & -1.48\text{e-}3 & +4.56\text{e-}2 \\
+3.53\text{e-}4 & +4.19\text{e-}4 & +7.06\text{e-}4 & +3.96\text{e-}3 & +2.89\text{e-}3 & -1.41\text{e-}3 & +3.24\text{e-}3 \\
+3.94\text{e-}3 & +7.06\text{e-}4 & +5.48\text{e-}3 & +1.86\text{e-}2 & +4.67\text{e-}3 & -2.18\text{e-}3 & +4.57\text{e-}2 \\
+1.49\text{e-}2 & +3.96\text{e-}3 & +1.86\text{e-}2 & +2.02\text{e+}1 & +6.00\text{e-}2 & -4.52\text{e-}2 & +1.96\text{e-}1 \\
+2.57\text{e-}3 & +2.89\text{e-}3 & +4.67\text{e-}3 & +6.00\text{e-}2 & +2.92\text{e-}2 & -1.30\text{e-}2 & +2.15\text{e-}2 \\
-1.48\text{e-}3 & -1.41\text{e-}3 & -2.18\text{e-}3 & -4.52\text{e-}2 & -1.30\text{e-}2 & +2.11\text{e-}2 & -1.28\text{e-}2 \\
+4.56\text{e-}2 & +3.24\text{e-}3 & +4.57\text{e-}2 & +1.96\text{e-}1 & +2.15\text{e-}2 & -1.28\text{e-}2 & +1.86\text{e+}0
\end{pmatrix}$$

The precision on L improves as more data sets are combined

Cosmic ray parameter values and associated covariance matrix for BIG

Unstable secondary ^{10}Be allows to measure a magnetic halo size L of 4.5 ± 1 kpc

Weinrich+[2002.11406] & Weinrich+2004.00441]

2) Antinuclei production through coalescence

coalescence $\equiv$ fusion of $\bar{p}$ & $\bar{n}$ into $\bar{d}$, $\overline{^3\mathrm{He}}$ or $\overline{^4\mathrm{He}}$

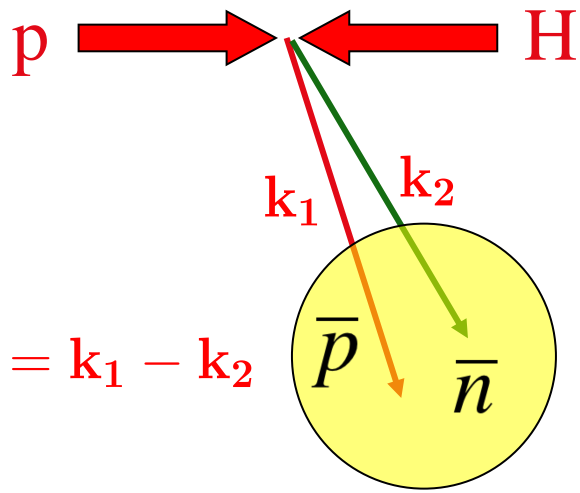

$$2\boldsymbol{\Delta} = \mathbf{k_1} - \mathbf{k_2} \qquad ||\boldsymbol{\Delta}|| \leq p_0$$

coalescence momentum $p_0 = p_{\rm coal}/2$

$$d^3\mathcal{N}_{\bar{d}}(\mathbf{K}) = \int d^6\mathcal{N}_{\bar{p},\bar{n}}\,\{\mathbf{k_1},\mathbf{k_2}\} \times \mathcal{C}(\boldsymbol{\Delta}) \text{ where } \mathbf{K} = \mathbf{k_1} + \mathbf{k_2}$$

$$B_2 = \frac{E_{\bar{d}}}{E_{\bar{p}}\,E_{\bar{n}}} \int d^3\boldsymbol{\Delta}\;\mathcal{C}(\boldsymbol{\Delta}) \simeq \frac{m_{\bar{d}}}{m_{\bar{p}}\,m_{\bar{n}}} \left\{ \frac{4}{3}\pi\, p_0^3 \equiv \frac{\pi}{6}\, p_{\rm coal}^3 \right\}$$

Coalescence factor B_2

$$\frac{E_{\bar{d}}}{\sigma_{\rm in}}\,\frac{d^3\sigma_{\bar{d}}}{d^3\mathbf{K}} = B_2 \left\{ \frac{E_{\bar{p}}}{\sigma_{\rm in}}\,\frac{d^3\sigma_{\bar{p}}}{d^3\mathbf{k_1}} \right\} \left\{ \frac{E_{\bar{n}}}{\sigma_{\rm in}}\,\frac{d^3\sigma_{\bar{n}}}{d^3\mathbf{k_2}} \right\}$$

2) Antinuclei production through coalescence

coalescence $\equiv$ fusion of $\bar{p}$ & $\bar{n}$ into $\bar{d}$, $\overline{^3\mathrm{He}}$ or $\overline{^4\mathrm{He}}$

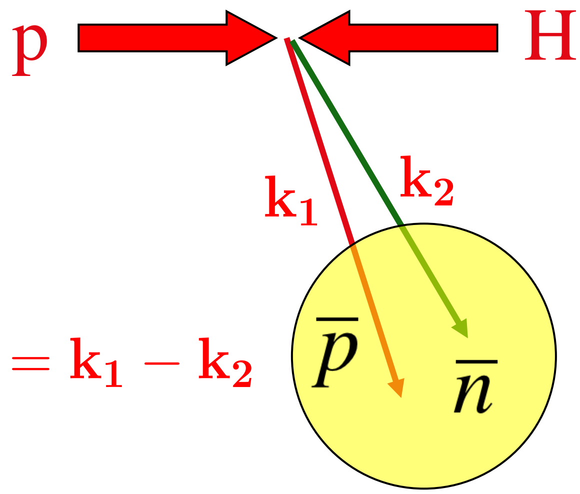

$$2\boldsymbol{\Delta} = \mathbf{k_1} - \mathbf{k_2} \qquad ||\boldsymbol{\Delta}|| \leq p_0$$

coalescence momentum $p_0 = p_{\rm coal}/2$

Production on anti-nuclei with mass A

$$\frac{E_{\bar{A}}}{\sigma_{\rm in}} \frac{d^3\sigma_{\bar{A}}}{d^3\boldsymbol{k}_{\bar{A}}} = B_A \left\{ \frac{E_{\bar{p}}}{\sigma_{\rm in}} \frac{d^3\sigma_{\bar{p}}}{d^3\boldsymbol{k}_{\bar{p}}} \right\}^Z \left\{ \frac{E_{\bar{n}}}{\sigma_{\rm in}} \frac{d^3\sigma_{\bar{n}}}{d^3\boldsymbol{k}_{\bar{n}}} \right\}^{A-Z} \quad \text{with} \quad \boldsymbol{k}_{\bar{p}} = \boldsymbol{k}_{\bar{n}} = \boldsymbol{k}_{\bar{A}}/A$$

Coalescence factor B_A

$$B_A = \frac{m_A}{m_p^Z m_n^{A-Z}} \left\{ \frac{\pi}{6} p_{\rm coal}^3 \right\}^{A-1}$$

2) Antinuclei production through coalescence

- ALICE provides an **experimental** determination of B_2 and B_3.
  $\bar{p}$ production cross-section is **measured**.
  Approximately the same value for p_0 from $\bar{d}$, $\bar{t}$ and $^3\overline{\mathrm{He}}$.

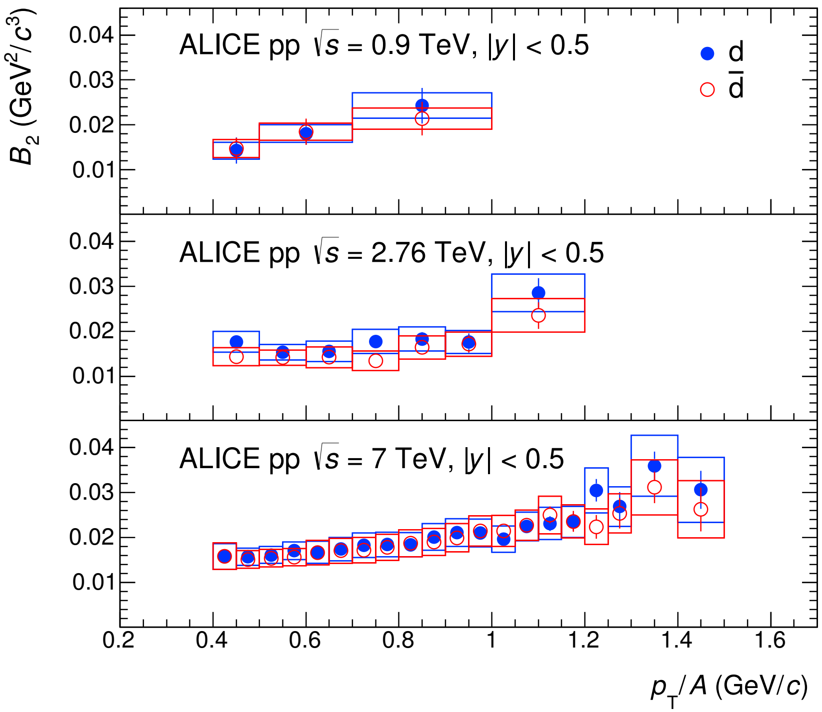

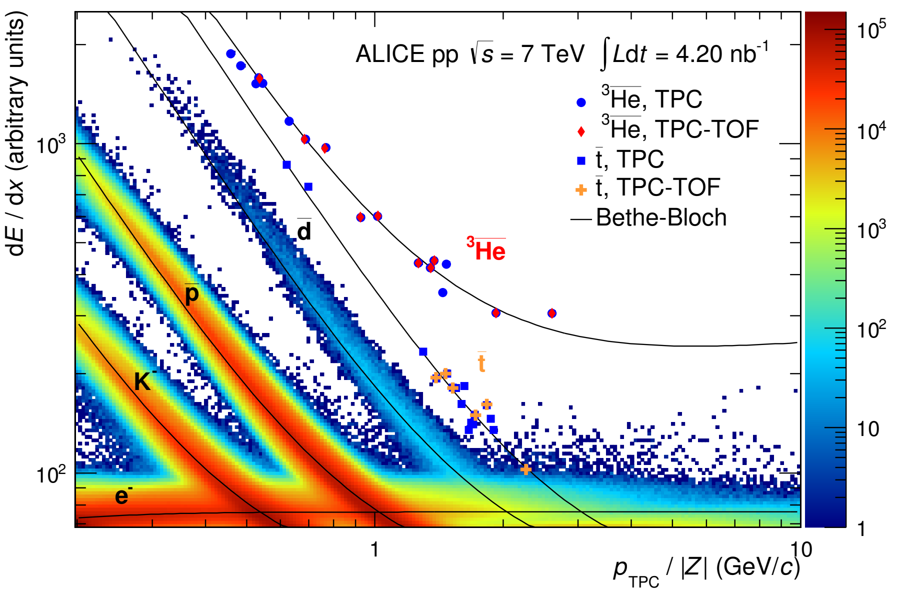

S. Acharya et al., Phys. Rev. **C97** (2018) 024615

2) Antinuclei production through coalescence

- ALICE provides an **experimental** determination of B_2 and B_3.
  $\bar{p}$ production cross-section is **measured**.
  Approximately the same value for p_0 from $\bar{d}$, $\bar{t}$ and $^3\overline{\mathrm{He}}$.

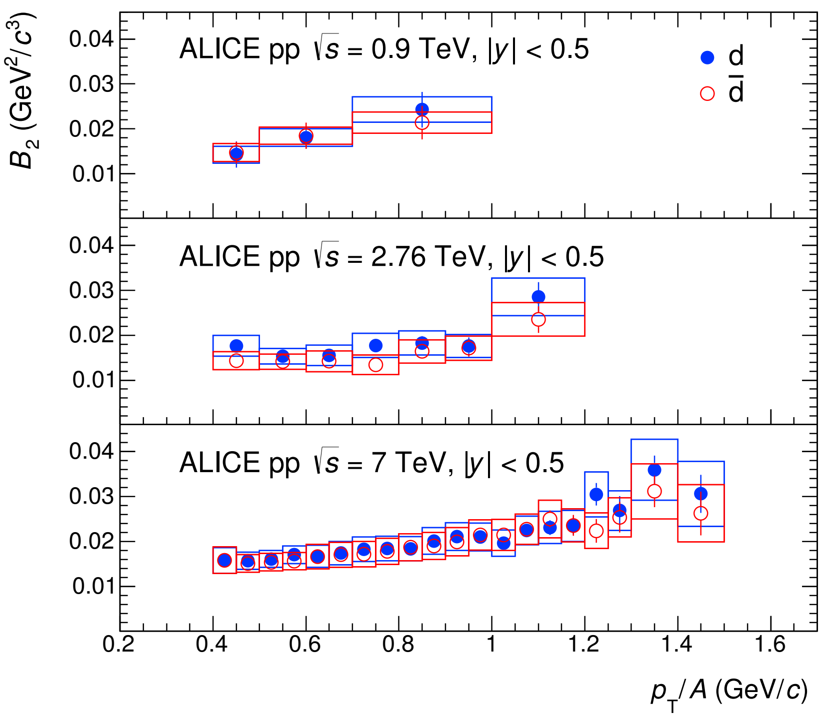

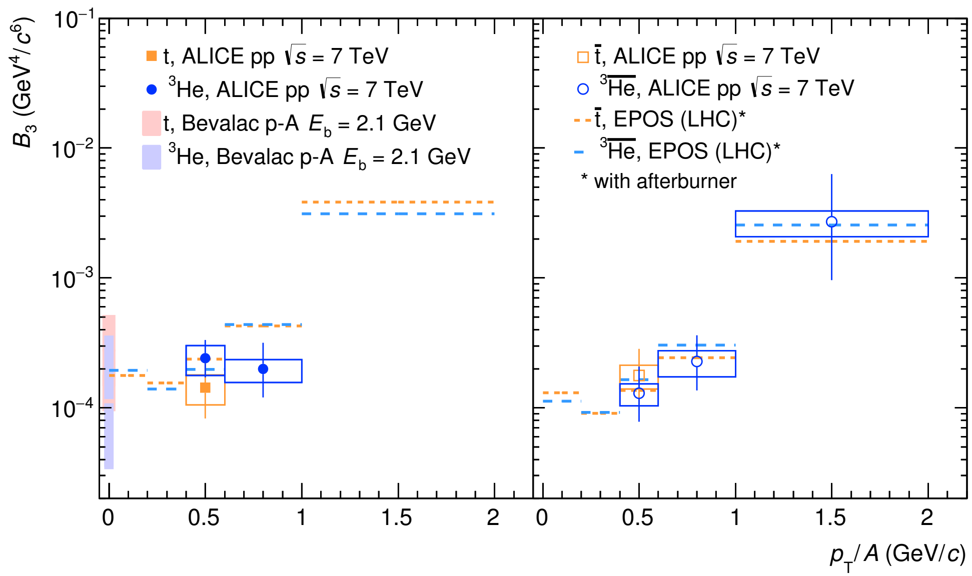

$208 \text{ MeV} \leq p_{\text{coal}} \leq 262 \text{ MeV}$

$218 \text{ MeV} \leq p_{\text{coal}} \leq 262 \text{ MeV}$

S. Acharya et al., Phys. Rev. **C97** (2018) 024615

2) Antinuclei production through coalescence

$$q_{\rm sec}(\bar{\rm A}\,|\,E_{\bar{\rm A}},\boldsymbol{x}) = \sum_{i\in{\rm p},\alpha}\ \sum_{j\in{\rm H,He}} 4\,\pi \int dE_i\ \Phi_i(E_i,\boldsymbol{x})\,n_j(\boldsymbol{x})\,\frac{d\sigma_{ij\to\bar{\rm A}}}{dE_{\bar{\rm A}}}(E_i,E_{\bar{\rm A}})$$

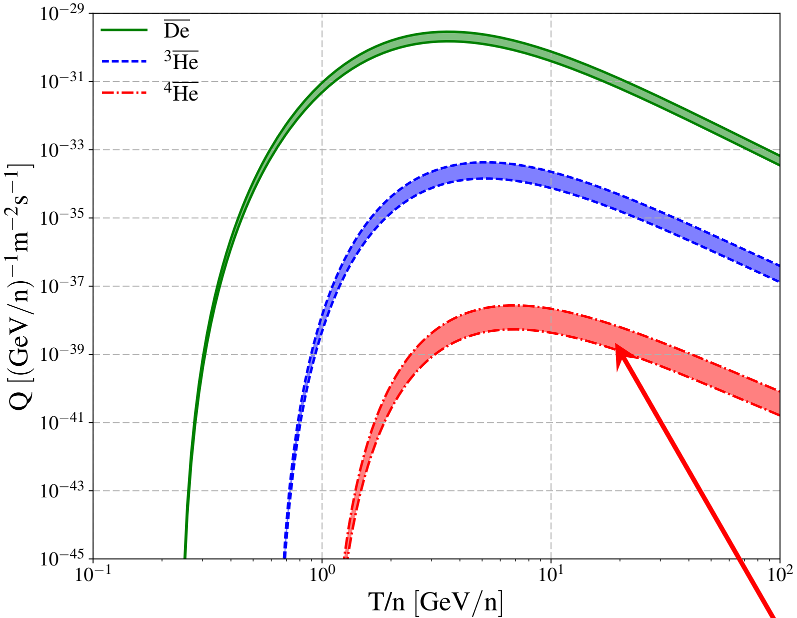

V. Poulin et al., Phys. Rev. **D99** (2019) 023016

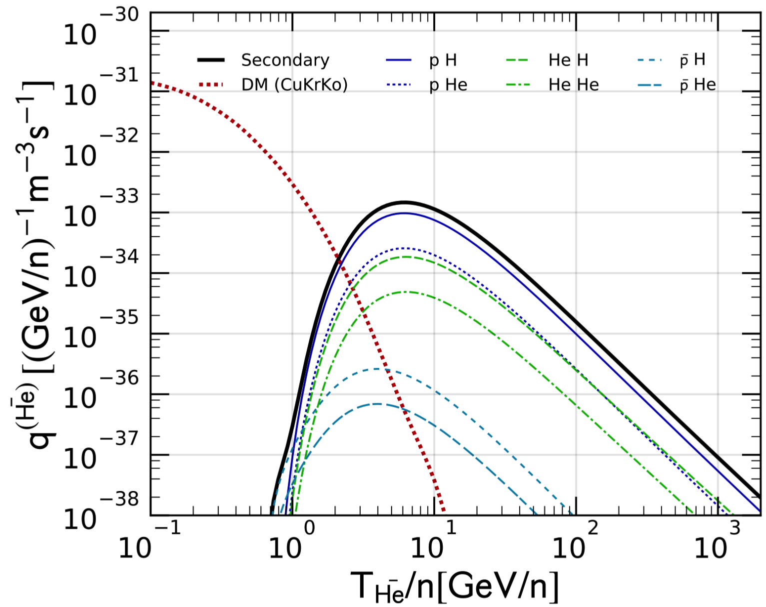

M. Korsmeier et al., Phys. Rev. **D97** (2018) 103011

$$7.7\times 10^{-7} \le \frac{B_4}{\rm GeV^6} \le 3.9\times 10^{-6}$$

$\bar{p}$ production modeled as in
M. di Mauro et al., Phys. Rev. **D90** (2014) 085017

2) Antinuclei production through coalescence

$$q_{\rm DM}(\bar{\rm A}\,|\,E_{\bar{\rm A}},\boldsymbol{x}) = \frac{1}{2}\left\{\frac{\rho_{\rm DM}(\boldsymbol{x})}{m_{\rm DM}}\right\}^2 \sum_{\rm channel\,F} \langle\sigma_{\rm ann}v\rangle_{\rm F} \times \frac{d\mathcal{N}_{\bar{\rm A}}^{\rm F}}{dE_{\bar{\rm A}}}$$

- Coalescence proceeds with the same pattern for DM annihilation. In the CMF of DM annihilation, the antinuclei $\bar{\rm A}$ multiplicity is

$$\frac{d\mathcal{N}_{\bar{\rm A}}}{dE_{\bar{\rm A}}} = B_A \left\{\frac{A^A}{(4\pi k_{\bar{\rm A}})^{A-1}}\right\} \sum_{\rm channel\,F} \mathcal{B}_{\rm F} \left\{\frac{d\mathcal{N}_{\bar{p}}^{\rm F}}{dE_{\bar{p}}}\right\}^Z \left\{\frac{d\mathcal{N}_{\bar{n}}^{\rm F}}{dE_{\bar{n}}}\right\}^{A-Z}$$

  where the multiplicities $d\mathcal{N}_{\bar{p}}/dE_{\bar{p}}$ and $d\mathcal{N}_{\bar{n}}/dE_{\bar{n}}$ are taken at $E_{\bar{p}} = E_{\bar{n}} = E_{\bar{\rm A}}/A$. The branching ratio to channel F is defined as $\mathcal{B}_{\rm F} = \langle\sigma_{\rm ann}v\rangle_{\rm F}/\langle\sigma_{\rm ann}v\rangle_{\rm tot}$.

- The coalescence scheme **does not** take into account angular correlations between antinucleons of the final state. Such correlations can be taken into account using an event-by-event coalescence model.

  Collisions and mostly DM annihilations can be simulated with a Monte-Carlo. generator. A coalescence condition is applied on the antinucleons of each event. In the CMF of the A final antinucleons, we require that each antinucleon fulfills

$$||\boldsymbol{p}_i^*|| < (A-1)^{1/(3A-3)} \left\{\frac{p_{\rm coal}}{2}\right\}$$

M. Winkler and T. Linden, Phys. Rev. Lett. **126** (2021) 101101

3) Antideuterons and the canonical approach

$$\frac{d\mathcal{N}_{\bar{d}}}{dE_{\bar{d}}} = \frac{m_{\bar{d}}}{m_{\bar{p}}\, m_{\bar{n}}} \left\{ \frac{p^3_{\rm coal}}{6\, k_{\bar{d}}} \right\} \sum_{\rm channel\,F} \mathcal{B}_{\rm F}\, \frac{d\mathcal{N}^{\rm F}_{\bar{p}}}{dE_{\bar{p}}}\, \frac{d\mathcal{N}^{\rm F}_{\bar{n}}}{dE_{\bar{n}}} \; @ \; E_{\bar{p}} = E_{\bar{n}} = E_{\bar{d}}/2$$

As shown in F. Donato et al., Phys. Rev. **D 62** (2000) 043003, DM antideuterons are to be found at low energy where the flux of antideuterons produced by cosmic ray primaries colliding on the ISM is deficient for kinematic reasons.

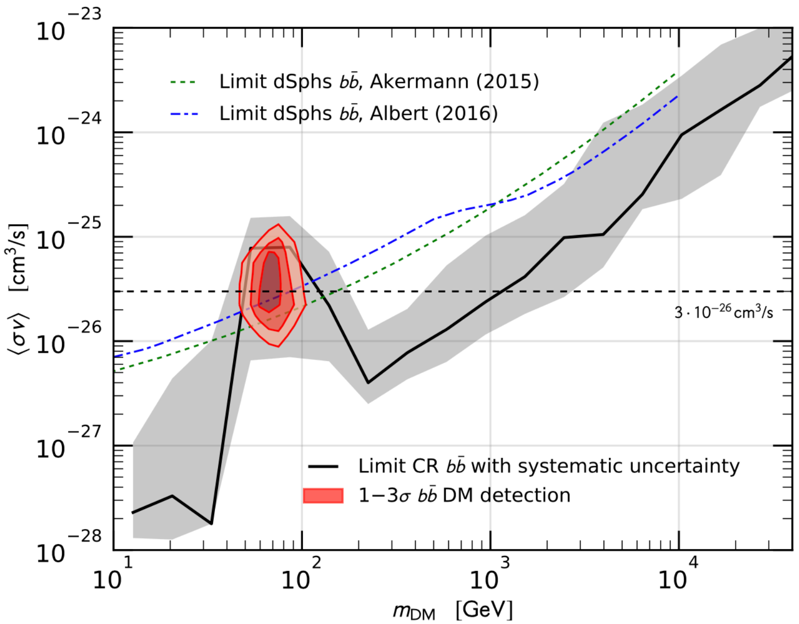

A. Cuoco et al., Phys. Rev. Lett. **118** (2017) 191102

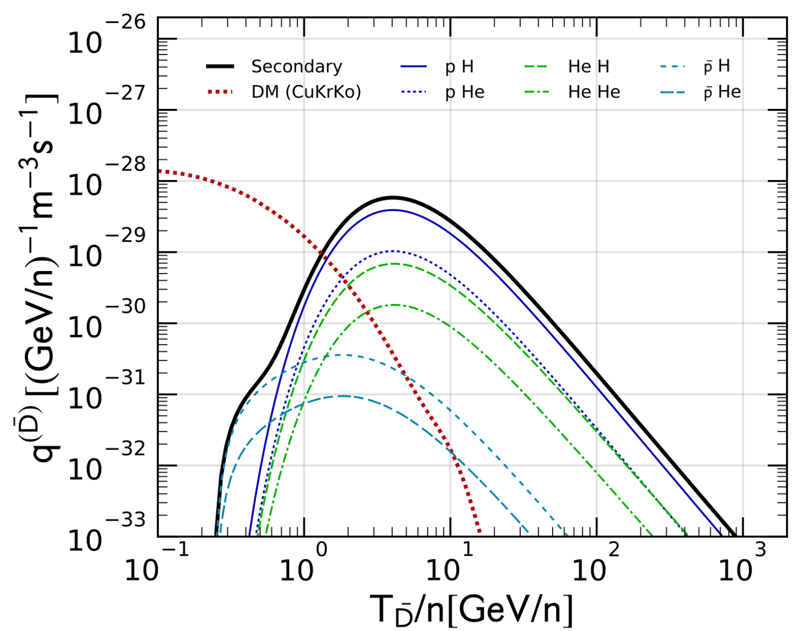

M. Korsmeier et al., Phys. Rev. **D97** (2018) 103011

3) Antideuterons and the canonical approach

$$\frac{d\mathcal{N}_{\bar d}}{dE_{\bar d}} = \frac{m_{\bar d}}{m_{\bar p}\, m_{\bar n}} \left\{ \frac{p_{\rm coal}^3}{6\, k_{\bar d}} \right\} \sum_{\rm channel\,F} \mathcal{B}_{\rm F} \, \frac{d\mathcal{N}_{\bar p}^{\rm F}}{dE_{\bar p}} \, \frac{d\mathcal{N}_{\bar n}^{\rm F}}{dE_{\bar n}} \;@\; E_{\bar p} = E_{\bar n} = E_{\bar d}/2$$

As shown in F. Donato et al., Phys. Rev. **D 62** (2000) 043003, DM antideuterons are to be found at low energy where the flux of antideuterons produced by cosmic ray primaries colliding on the ISM is deficient for kinematic reasons.

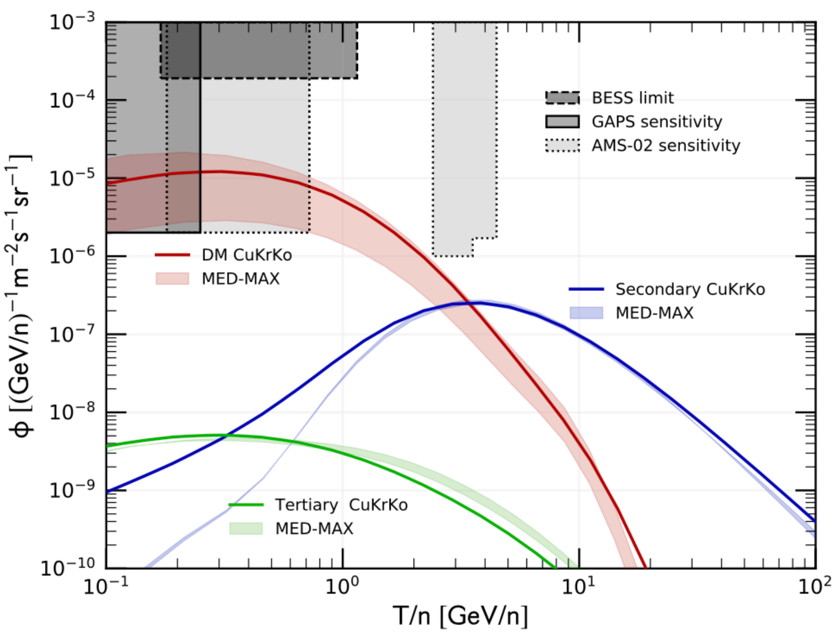

$p_{\rm coal} = 160$ MeV

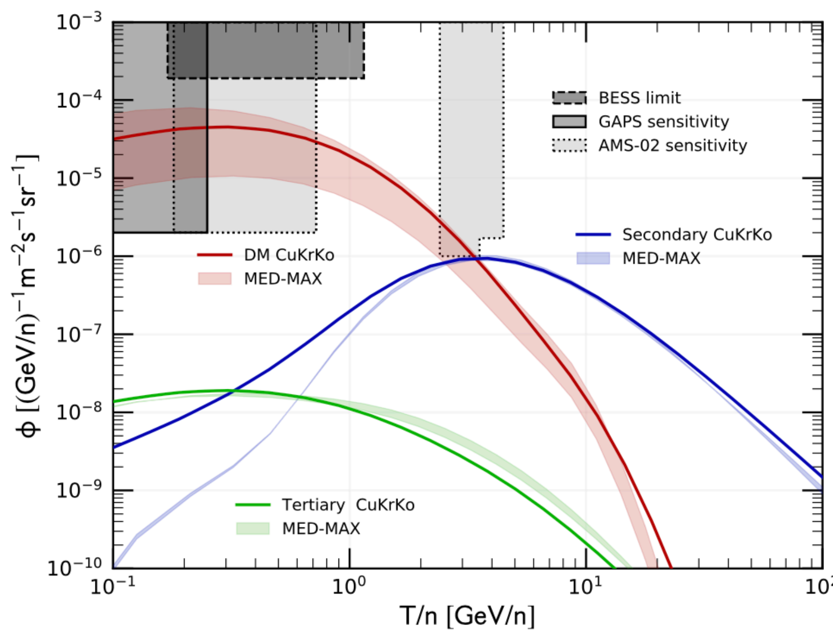

$p_{\rm coal} = 248$ MeV

M. Korsmeier et al., Phys. Rev. **D97** (2018) 103011

4) Exotic scenarios for antihelium DM production

$$\frac{d\mathcal{N}_{\overline{\mathrm{He}}}}{dE_{\overline{\mathrm{He}}}} = \frac{3\, m_{\overline{\mathrm{He}}}}{m_{\bar{p}}^2\, m_{\bar{n}}} \left\{ \frac{p_{\mathrm{coal}}^3}{8\, k_{\overline{\mathrm{He}}}} \right\}^2 \sum_{\mathrm{channel\,F}} \mathcal{B}_{\mathrm{F}} \left\{ \frac{d\mathcal{N}_{\bar{p}}^{\mathrm{F}}}{dE_{\bar{p}}} \right\}^2 \frac{d\mathcal{N}_{\bar{n}}^{\mathrm{F}}}{dE_{\bar{n}}} \;@\; E_{\bar{p}} = E_{\bar{n}} = E_{\overline{\mathrm{He}}}/3$$

- Interactions of high-energy cosmic-ray protons and helium nuclei on the ISM yield a **secondary anti-He flux** well below AMS-02 sensitivity.
- The same conclusion holds for DM decays or annihilations in canonical models where the production occurs at the DM vertex. But stay tuned!

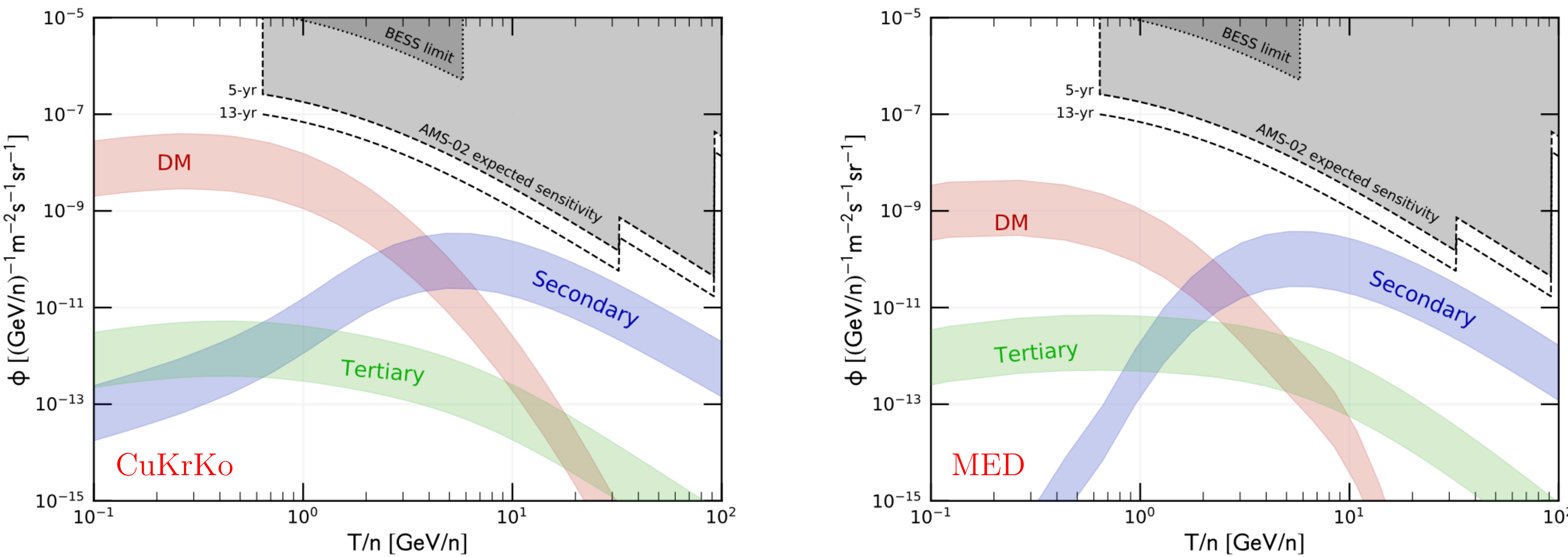

M. Korsmeier et al., Phys. Rev. **D97** (2018) 103011

4) $^3\overline{\mathrm{He}}$ nuclei and beautiful dark matter

- A new idea has been proposed based on DM annihilating into b quarks.
- The $b\bar{b}$ colored string has a non-vanishing probability to yield a $\bar{\Lambda}_b$ baryon. This has been observed at LEP.
- Antinucleons are produced at the annihilating DM vertex (prompt) and also at the displaced in-flight $\bar{\Lambda}_b$ decay vertex.

$$\chi + \chi \rightarrow b + \bar{b} \qquad \bar{b} \rightarrow \bar{\Lambda}_b \text{ baryon } (\bar{b}\bar{u}\bar{d})$$

$$\bar{\Lambda}_b\,(5.6\ \text{GeV}) \rightarrow {}^3\overline{\text{He}} + 2p\,(4.7\ \text{GeV})$$

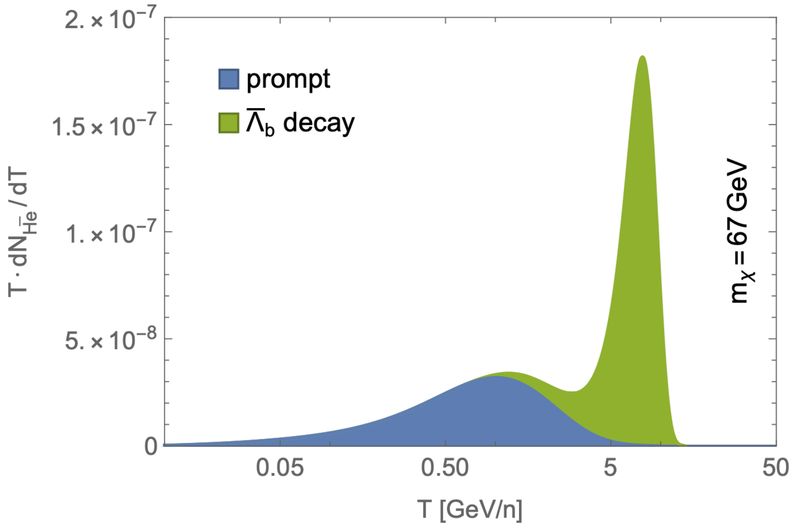

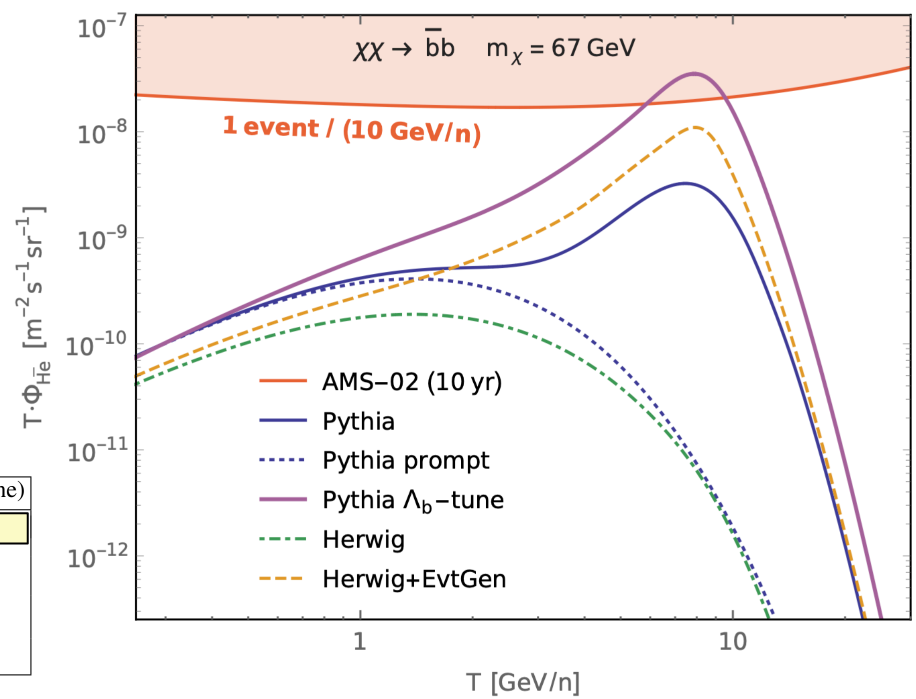

experiment	channel	measurement	Pythia (default)	Pythia (Λ_b-tune)
LEP [4, 5]	$f(b \rightarrow \Lambda_b)$	$0.101^{+0.039}_{-0.031}$	0.037	0.101
LEP [6]	$f(b \rightarrow \Lambda_b, \Xi_b, \Omega_b)$	0.117 ± 0.021	0.047	0.127
Tevatron CDF [7]	$\frac{f(b\rightarrow\Lambda_b)}{f(b\rightarrow B)}$	$0.281^{+0.141}_{-0.103}$	0.046	0.135
LHCb [8]	$\frac{f(b\rightarrow\Lambda_b)}{f(b\rightarrow B)}$	0.259 ± 0.018	0.048	0.134

M. Winkler and T. Linden, Phys. Rev. Lett. **126** (2021) 101101

Counterarguments – Kachelriess+[2105.00799]

- To get the value of $f(b \to \Lambda_b)$ measured at LEP, WL21 have increased the probability `probQQtoQ` for diquark formation in hadronization from 0.09 to 0.24, playing havoc with other processes.

- This implies:
(i) an over production of protons and antiprotons at LEP by a factor of 2,
(ii) an increase in proton yield with respect to kaon and pion yields $dN/dy|_{|y|<0.5}$ measured by ALICE at LHC.

- In default Pythia, $\mathrm{Br}(\bar{\Lambda}_b \to \overline{^3\mathrm{He}}) \simeq 3 \times 10^{-6}$ may already be too large. Default Pythia overestimates branching ratios for several Λ_b decay channels. Mismodeling of diquark formation.

$\sqrt{s}$	≈ 10 GeV	29–35 GeV	91 GeV	130–200 GeV
Obs.	0.266 ± 0.008	0.640 ± 0.050	1.050 ± 0.032	1.41 ± 0.18
WL21	0.640	1.161	2.102	2.33

p and $\bar{p}$ multiplicity in e^+e^- annihilations

Particle	proton	kaon	pion
dN/dy, LHC	0.124 ± 0.009	0.286 ± 0.016	2.26 ± 0.10
dN/dy, Λ_b tune	0.328	0.231	1.90

dN/dy at mid-rapidity $|y| < 0.5$
at LHC at $\sqrt{s} = 7$ TeV for p, K^+ and π^+

Branching ratio	PDG	Pythia
$\Lambda_b \to \Lambda_c^+ p\bar{p}\pi^-$	2.65×10^{-4}	1.5×10^{-3}
$\Lambda_b \to \Lambda_c^+ \pi^+\pi^-\pi^-$	7.7×10^{-3}	0.047
$\Lambda_b \to \Lambda\pi^+\pi^-$	4.7×10^{-6}	2.0×10^{-5}
$\Lambda_b \to p\pi^-\pi^+\pi^-$	2.11×10^{-5}	9.6×10^{-5}
$\Lambda_b \to pK^-K^+\pi^-$	4.1×10^{-6}	1.7×10^{-5}
$B^0 \to p\bar{p}K^0$	2.66×10^{-6}	6.1×10^{-6}
$B^0 \to p\bar{p}\pi^+\pi^-$	2.87×10^{-6}	5.6×10^{-6}
$B^0 \to \Lambda_c^- p\pi^+\pi^-$	1.02×10^{-3}	2.1×10^{-3}
$\Lambda_c \to p\pi^+\pi^-$	4.61×10^{-3}	0.012
$\Lambda_c \to p\pi^0$	$< 2.7 \times 10^{-4}$	2.0×10^{-3}
$\Lambda_c \to \Lambda K^+\pi^+\pi^-$	$< 5 \times 10^{-4}$	2.1×10^{-3}

Let us measure $\mathrm{Br}(\bar{\Lambda}_b \to \overline{^3\mathrm{He}})$ and see!

Counterarguments – Kachelriess+[2105.00799]

- To get the value of $f(b \to \Lambda_b)$ measured at LEP, WL21 have increased the probability `probQQtoQ` for diquark formation in hadronization from 0.09 to 0.24, playing havoc with other processes.

- This implies:
(i) an over production of protons and antiprotons at LEP by a factor of 2,
(ii) an increase in proton yield with respect to kaon and pion yields $dN/dy|_{|y|<0.5}$ measured by ALICE at LHC.

- In default Pythia, $\mathrm{Br}(\bar{\Lambda}_b \to \overline{^3\mathrm{He}}) \simeq 3 \times 10^{-6}$ may already be too large. Default Pythia overestimates branching ratios for several Λ_b decay channels. Mismodeling of diquark formation.

$\sqrt{s}$	≈ 10 GeV	29–35 GeV	91 GeV	130–200 GeV
Obs.	0.266 ± 0.008	0.640 ± 0.050	1.050 ± 0.032	1.41 ± 0.18
WL21	0.640	1.161	2.102	2.33

p and $\bar{p}$ multiplicity in e^+e^- annihilations

Particle	proton	kaon	pion
dN/dy, LHC	0.124 ± 0.009	0.286 ± 0.016	2.26 ± 0.10
dN/dy, Λ_b tune	0.328	0.231	1.90

dN/dy at mid-rapidity $|y| < 0.5$
at LHC at $\sqrt{s} = 7$ TeV for p, K^+ and π^+

Branching ratio	PDG	Pythia
$\Lambda_b \to \Lambda_c^+ p\bar{p}\pi^-$	2.65×10^{-4}	1.5×10^{-3}
$\Lambda_b \to \Lambda_c^+ \pi^+\pi^-\pi^-$	7.7×10^{-3}	0.047
$\Lambda_b \to \Lambda\pi^+\pi^-$	4.7×10^{-6}	2.0×10^{-5}
$\Lambda_b \to p\pi^-\pi^+\pi^-$	2.11×10^{-5}	9.6×10^{-5}
$\Lambda_b \to pK^-K^+\pi^-$	4.1×10^{-6}	1.7×10^{-5}
$B^0 \to p\bar{p}K^0$	2.66×10^{-6}	6.1×10^{-6}
$B^0 \to p\bar{p}\pi^+\pi^-$	2.87×10^{-6}	5.6×10^{-6}
$B^0 \to \Lambda_c^- p\pi^+\pi^-$	1.02×10^{-3}	2.1×10^{-3}
$\Lambda_c \to p\pi^+\pi^-$	4.61×10^{-3}	0.012
$\Lambda_c \to p\pi^0$	$< 2.7 \times 10^{-4}$	2.0×10^{-3}
$\Lambda_c \to \Lambda K^+\pi^+\pi^-$	$< 5 \times 10^{-4}$	2.1×10^{-3}

$\mathrm{Br}(\bar{\Lambda}_b \to \overline{^3\mathrm{He}} + X) < 6.3 \times 10^{-8}$ @ 90% CL

4) $^3\overline{\text{He}}$ nuclei and beautiful dark matter

- Antinuclei production in cosmic ray collisions on the ISM are modeled using the analytic coalescence model. Values of the coalescence momenta are extracted from accelerator data.

$$p_{\text{coal}}(\bar{d}) = 208 \pm 26\,\text{MeV} \;\text{ while }\; p_{\text{coal}}(^3\overline{\text{He}}) = 238 \pm 30\,\text{MeV}$$

- Antinuclei production in DM annihilation is simulated with Pythia 8.3 coupled to an event-by-event coalescence model. The $\bar{\Lambda}_b$-induced fluxes are rescaled by a factor of 2.8.
- The DM model is based on a recent fit of cosmic ray nuclei and antiproton data – see P. De La Torre Luque at al., arXiv:2404.13114 [astro-ph.HE].

$$m_{\text{DM}} = 66.3\,\text{GeV} \;\text{and}\; \langle \sigma_{\text{ann}} v \rangle \simeq 10^{-26}\,\text{cm}^3\text{s}^{-1} \;\text{through}\; b\bar{b} \;\text{channel}$$

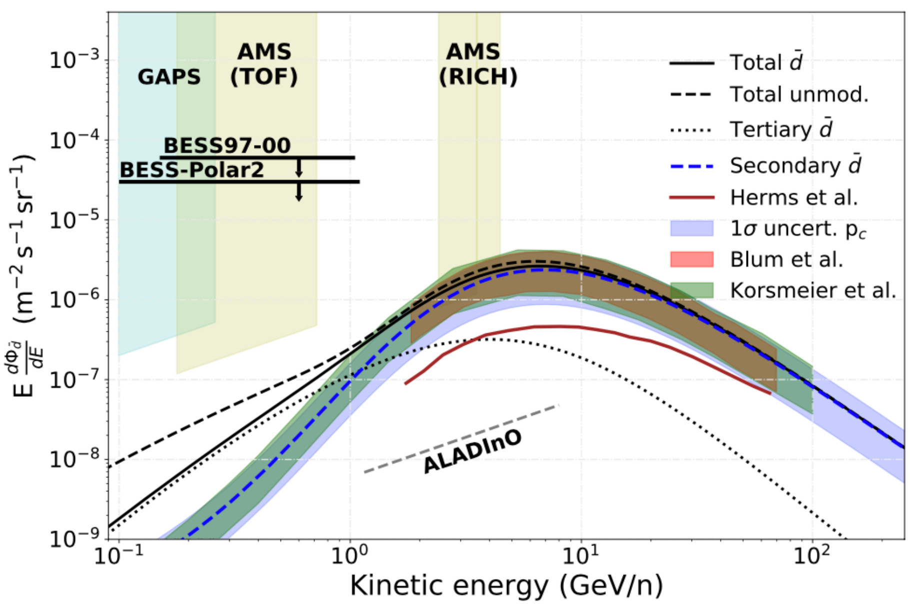

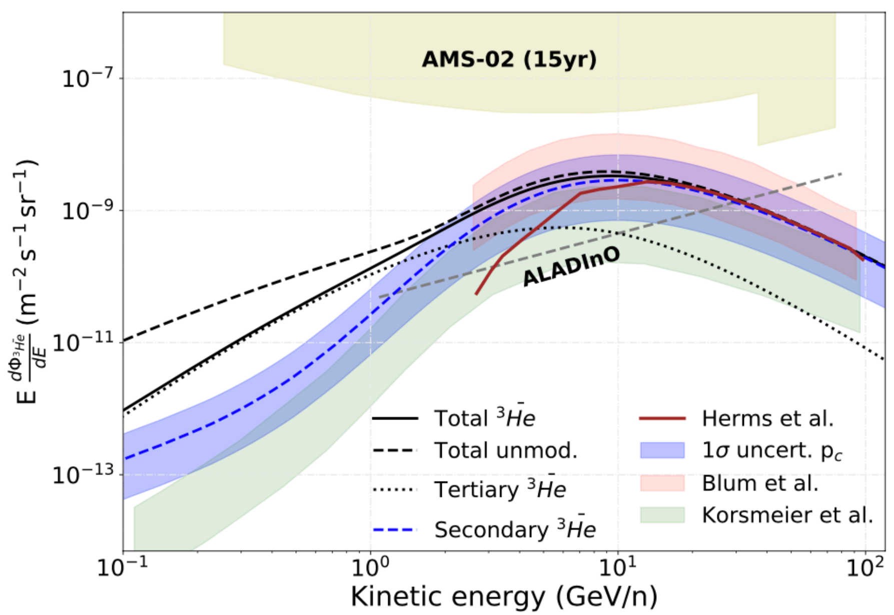

4) $^3\overline{\text{He}}$ nuclei and beautiful dark matter

- Antinuclei production in cosmic ray collisions on the ISM are modeled using the analytic coalescence model. Values of the coalescence momenta are extracted from accelerator data.

$$p_{\rm coal}(\bar{d}) = 208 \pm 26\,\text{MeV while } p_{\rm coal}(^3\overline{\text{He}}) = 238 \pm 30\,\text{MeV}$$

- Antinuclei production in DM annihilation is simulated with Pythia 8.3 coupled to an event-by-event coalescence model. The $\bar{\Lambda}_b$-induced fluxes are rescaled by a factor of 2.8.
- The DM model is based on a recent fit of cosmic ray nuclei and antiproton data – see P. De La Torre Luque at al., arXiv:2404.13114 [astro-ph.HE].

$$m_{\rm DM} = 66.3\,\text{GeV and } \langle \sigma_{\rm ann} v \rangle \simeq 10^{-26}\,\text{cm}^3\text{s}^{-1} \text{ through } b\bar{b} \text{ channel}$$

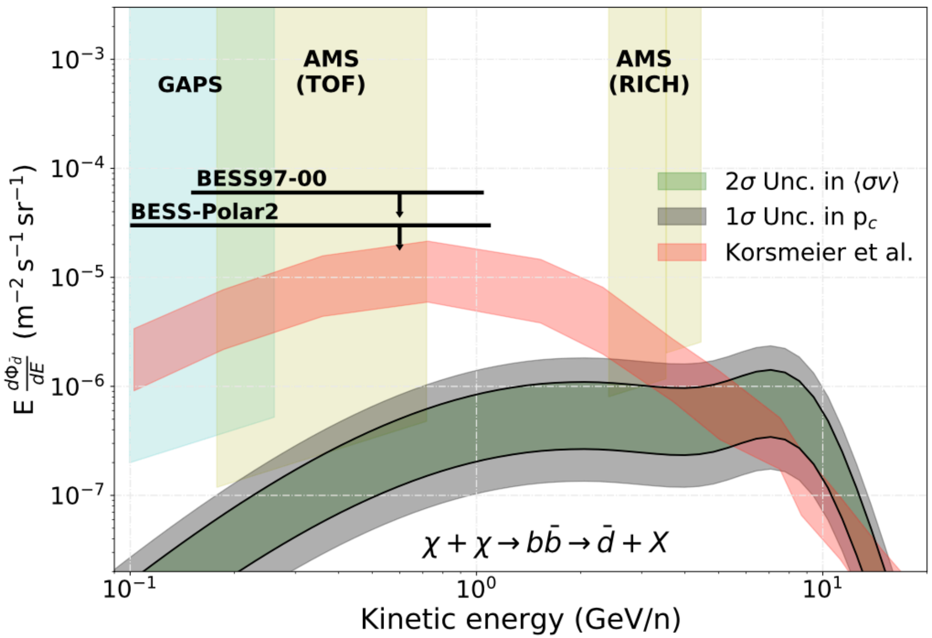

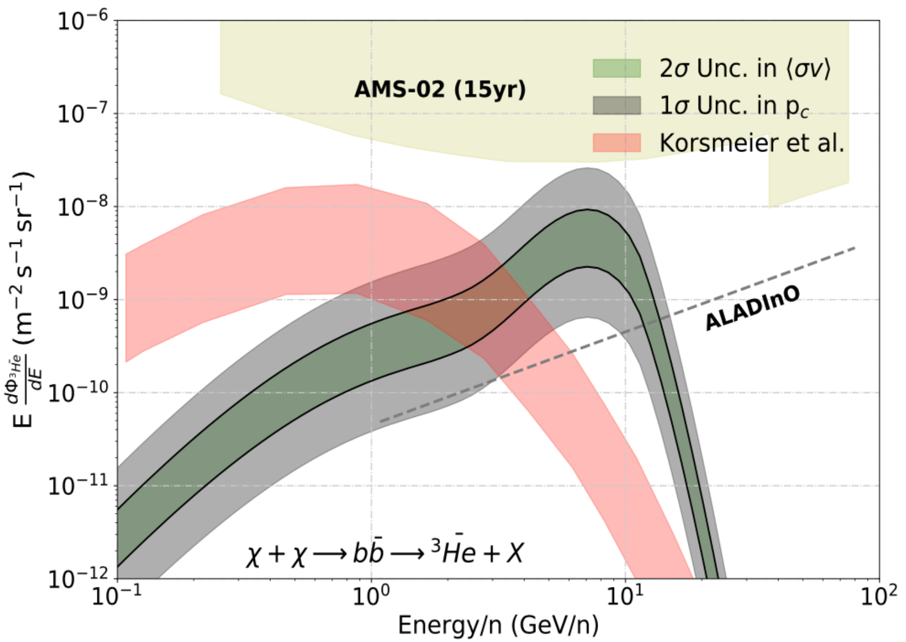

4) $^4\overline{\mathrm{He}}$ nuclei, truth and cosmic hedgehogs

Production on anti-nuclei with mass A

$$\frac{d\mathcal{N}_{\bar{\mathrm{A}}}}{dE_{\bar{\mathrm{A}}}} = B_A \left\{ \frac{A^A}{(4\pi k_{\bar{\mathrm{A}}})^{A-1}} \right\} \left\{ \frac{d\mathcal{N}_{\bar{p}}}{dE_{\bar{p}}} \right\}^Z \left\{ \frac{d\mathcal{N}_{\bar{n}}}{dE_{\bar{n}}} \right\}^{A-Z} \quad \text{with } \boldsymbol{k}_{\bar{p}} = \boldsymbol{k}_{\bar{n}} = \boldsymbol{k}_{\bar{A}}/A$$

(i) If $d\mathcal{N}_{\bar{p}}/dE_{\bar{p}}$ is enhanced by a factor λ, $d\mathcal{N}_{\bar{\mathrm{A}}}/dE_{\bar{\mathrm{A}}}$ should be enhanced by a factor λ^A.

(ii) In models where DM annihilates into Higgs pairs, subsequent hadronization of the $b\bar{b}$ pairs yields $\mathcal{O}(100)$ pions.

$$\chi\chi \to hh \to 2\bar{b}b \to \mathcal{O}(100)\,\pi$$

If DM is very heavy and coupled to a **dark QCD sector,** we can imagine the chain of reactions involving dark quarks, dark gluons and dark pions eventually yielding $\bar{t}t$ pairs.

$$\chi\chi \to \phi\phi \to 2\bar{q}'q' \to N_{\pi'}\,\pi' \to N_{\pi'}\,\bar{t}t$$

The **dark QCD** reactions can be modeled through the decay chain involving the scalars $\varphi_1, \varphi_2, \ldots, \varphi_n$ whose masses are fine-tuned with $m_{\varphi_i} = 2.01\, m_{\varphi_{i+1}}$.

$$\phi \to 2\varphi_1 \to 4\varphi_2 \to 2^n\varphi_n \to 2^{n+1}\pi' \to 2^{n+1}\bar{t}t$$

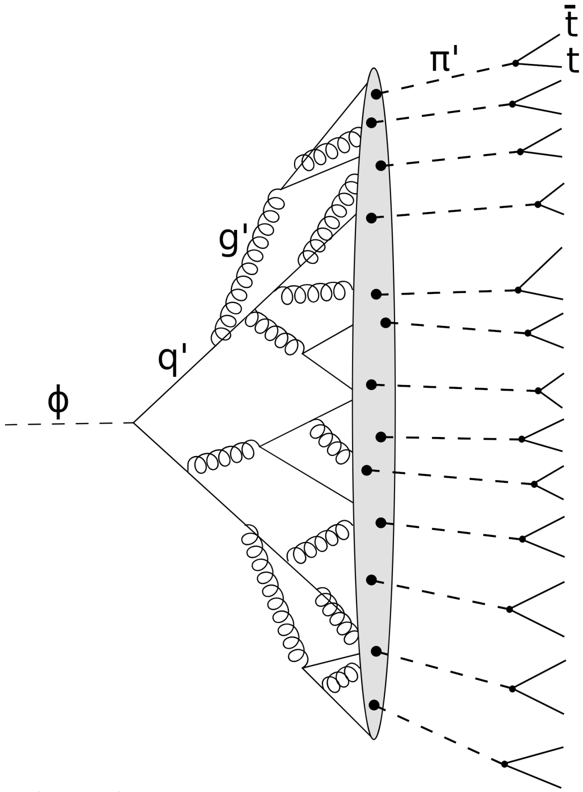

M. Winkler et al., Phys. Rev. **D107** (2023) 123035

4) $^4\overline{\mathrm{He}}$ nuclei, truth and cosmic hedgehogs

Production on anti-nuclei with mass A

$$\frac{d\mathcal{N}_{\bar{\mathrm{A}}}}{dE_{\bar{\mathrm{A}}}} = B_A \left\{ \frac{A^A}{(4\pi k_{\bar{\mathrm{A}}})^{A-1}} \right\} \left\{ \frac{d\mathcal{N}_{\bar{p}}}{dE_{\bar{p}}} \right\}^Z \left\{ \frac{d\mathcal{N}_{\bar{n}}}{dE_{\bar{n}}} \right\}^{A-Z} \text{ with } \boldsymbol{k}_{\bar{p}} = \boldsymbol{k}_{\bar{n}} = \boldsymbol{k}_{\bar{A}}/A$$

(i) If $d\mathcal{N}_{\bar{p}}/dE_{\bar{p}}$ is enhanced by a factor λ, $d\mathcal{N}_{\bar{\mathrm{A}}}/dE_{\bar{\mathrm{A}}}$ should be enhanced by a factor λ^A.

(ii) In models where DM annihilates into Higgs pairs, subsequent hadronization of the $b\bar{b}$ pairs yields $\mathcal{O}(100)$ pions.

$$\chi\chi \to hh \to 2\bar{b}b \to \mathcal{O}(100)\,\pi$$

If DM is very heavy and coupled to a **dark QCD sector,** we can imagine the chain of reactions involving dark quarks, dark gluons and dark pions eventually yielding $\bar{t}t$ pairs.

$$\chi\chi \to \phi\phi \to 2\bar{q}'q' \to N_{\pi'}\,\pi' \to N_{\pi'}\,\bar{t}t$$

The **dark QCD** reactions can be modeled through the decay chain involving the scalars φ_1, φ_2, ... , φ_n whose masses are fine-tuned with $m_{\varphi_i} = 2.01\, m_{\varphi_{i+1}}$.

$$\phi \to 2\varphi_1 \to 4\varphi_2 \to 2^n\varphi_n \to 2^{n+1}\pi' \to 2^{n+1}\bar{t}t$$

M. Winkler et al., Phys. Rev. **D107** (2023) 123035

4) $^4\overline{\text{He}}$ nuclei, truth and cosmic hedgehogs

DM type	Annihilating	Decaying
Input Parameters		
m_χ [TeV]	150	5000
m_ϕ [TeV]	50.4	375
$m_{\pi'}$ [GeV]	380	700
$N_{\pi'}$	256	1024
$\langle \sigma v \rangle$ [cm^{3}s^{-1}]	6.6×10^{-24}	–
Γ [s^{-1}]	–	9×10^{-30}
Antinuclei Events at AMS-02		
$^3\overline{\text{He}}$	15.6	20.3
$^4\overline{\text{He}}$	1.0	3.1
$\bar{\text{d}}$	19.3	1.2
Antinuclei Events at GAPS		
$\bar{\text{d}}$	0.7	0

TABLE I. Input parameters of one annihilating and one decaying DM benchmark scenario. Also given are the predicted antihelium and antideuteron event numbers at AMS-02 (per ten years) and GAPS.

$$\bar{\text{p}} : \bar{\text{d}} : {}^3\overline{\text{He}} : {}^4\overline{\text{He}} = 3 \times 10^4 : 3 \times 10^2 : 18 : 1$$

instead of the conventional ratios

$$\bar{\text{p}} : \bar{\text{d}} : {}^3\overline{\text{He}} : {}^4\overline{\text{He}} = 10^{10} : 10^7 : 10^4 : 1$$

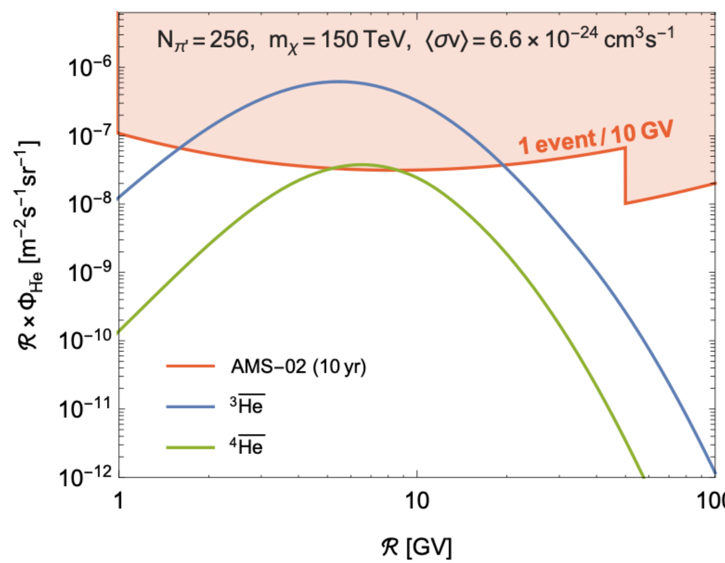

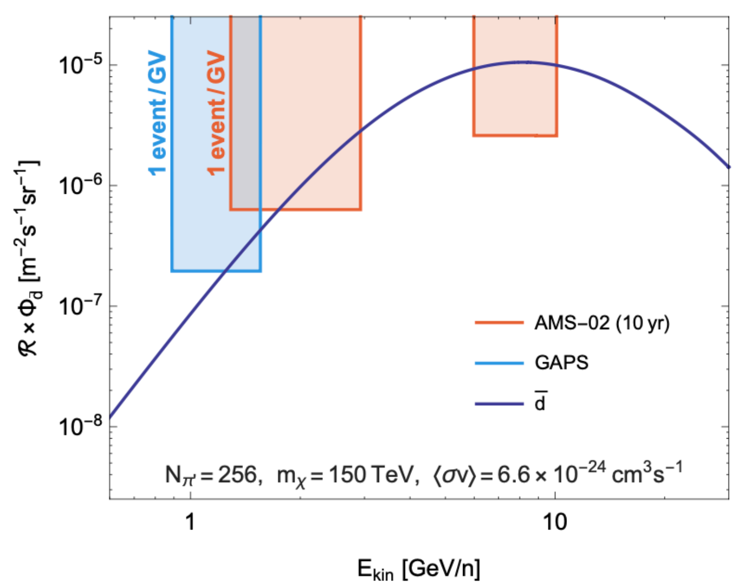

M. Winkler et al., Phys. Rev. **D107** (2023) 123035

The message from heavy ion collisions

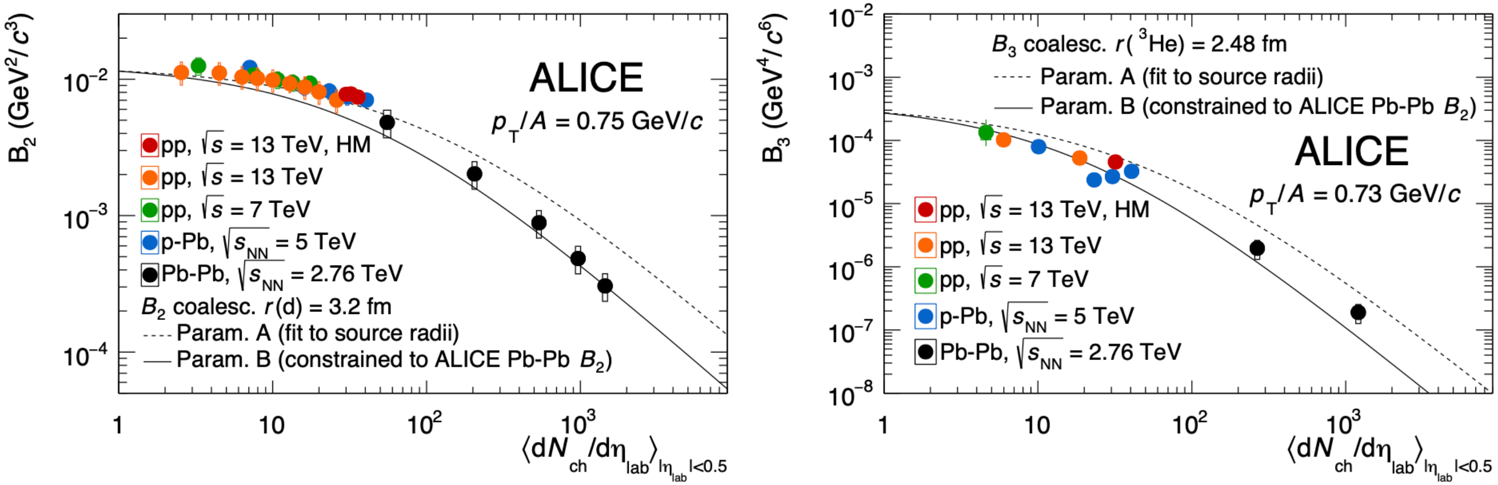

(a) (Anti)deuterons (b) (Anti)helions

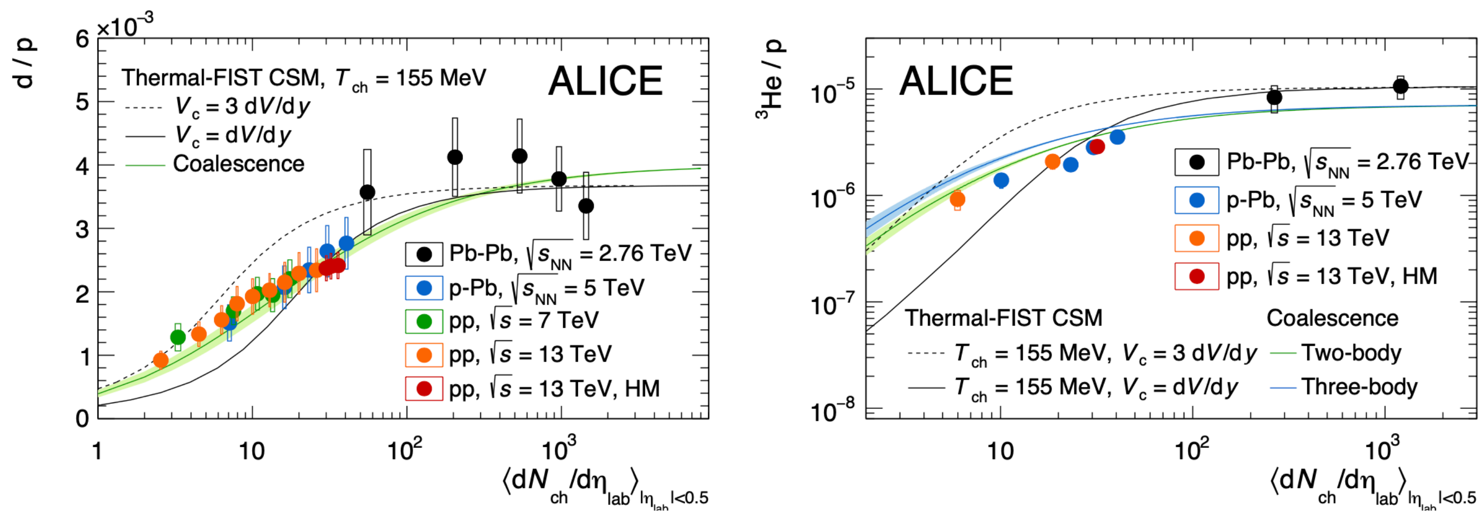

(a) (Anti)deuterons (b) (Anti)helions

The conventional hierarchy is not much modified when the multiplicity increases

S. Acharya et al., JHEP **01** (2022) 106

4) Antinucleosynthesis inside cosmic BSM fireballs

Assume isolated, catastrophic injections of large quantities of energetic SM anti-quarks in our Galaxy by BSM physics (yet to be determined)

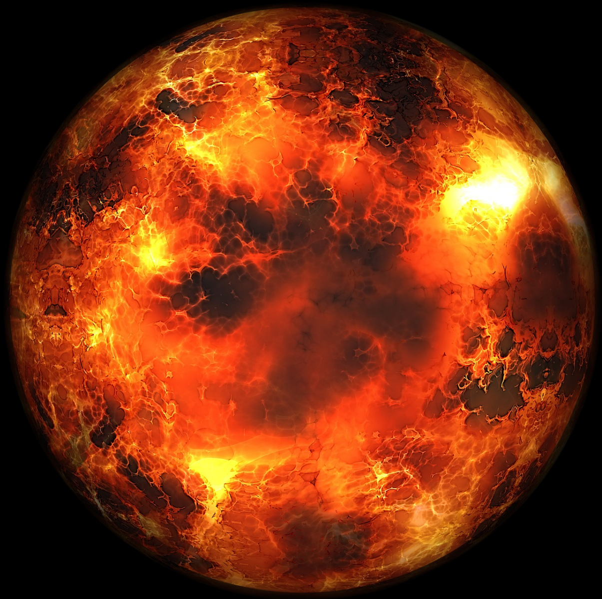

- R_0 between 0.1 mm and 1 m
- T_0 below $\Lambda_{\rm QCD} \sim 200\,\rm MeV$
- Antibaryon-to-photon ratio $\bar{\eta} \sim 10^{-2}$

M. Fedderke et al., Phys. Rev. **D109** (2024) 123028

4) Antinucleosynthesis inside cosmic BSM fireballs

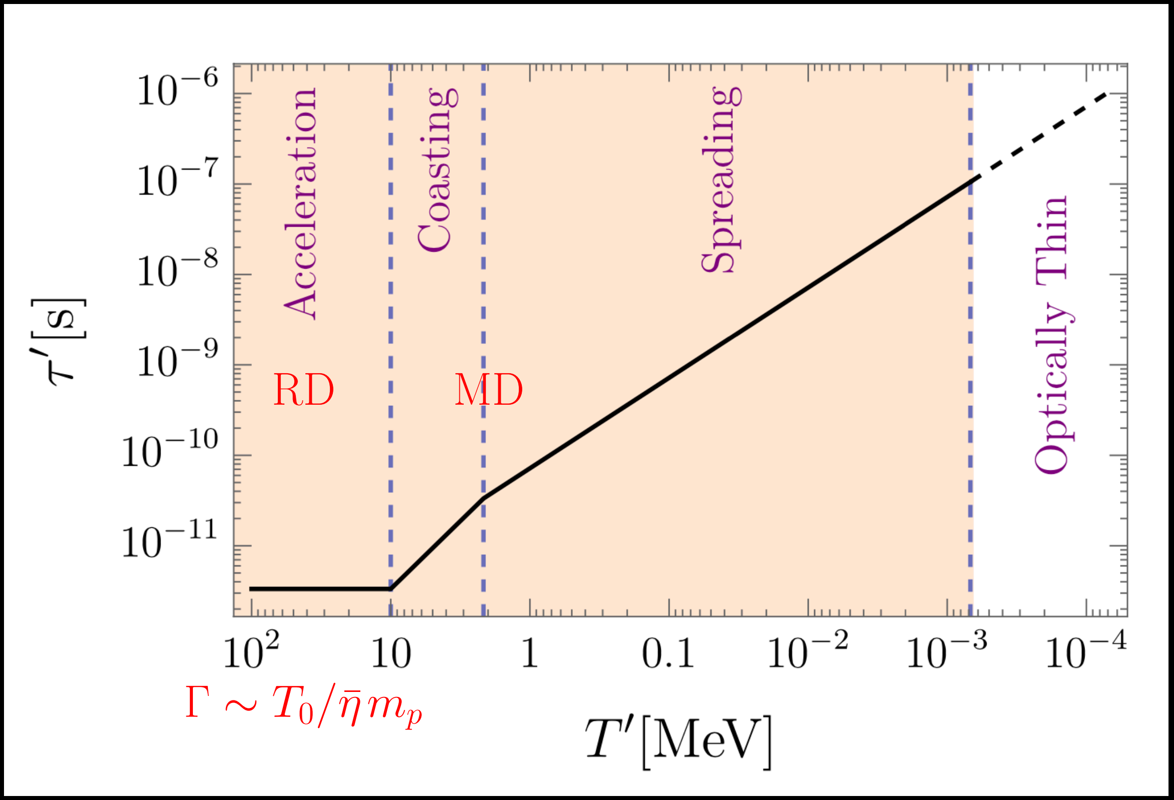

The comoving expansion timescale τ' is plotted as a function of the comoving temperature T' for a fireball with $T_0 = 100\,\mathrm{MeV}$, $R_0 = 1\,\mathrm{mm}$ and $\bar{\eta} = 10^{-2}$.

M. Fedderke et al., Phys. Rev. **D109** (2024) 123028

4) Antinucleosynthesis inside cosmic BSM fireballs

• Weak interactions are frozen given the short expansion timescale. $\bar{p}$ and $\bar{n}$ are transmuted into each other through the strong reactions

$$\bar{n} + \pi^- \leftrightarrow \bar{p} + \pi^0 \; (Q = 3.3\,\mathrm{MeV})$$

$$\bar{p} + \pi^+ \leftrightarrow \bar{n} + \pi^0 \; (Q = 5.9\,\mathrm{MeV}).$$

• The equilibrium between antiprotons and antineutrons freezes out at $T' \simeq 6$ to $8\,\mathrm{MeV}$.

• Nucleosynthesis starts when antideuterium stops to be photodissociated at $T' \simeq 140$ to $170\,\mathrm{keV}$ and takes place during the spreading phase.

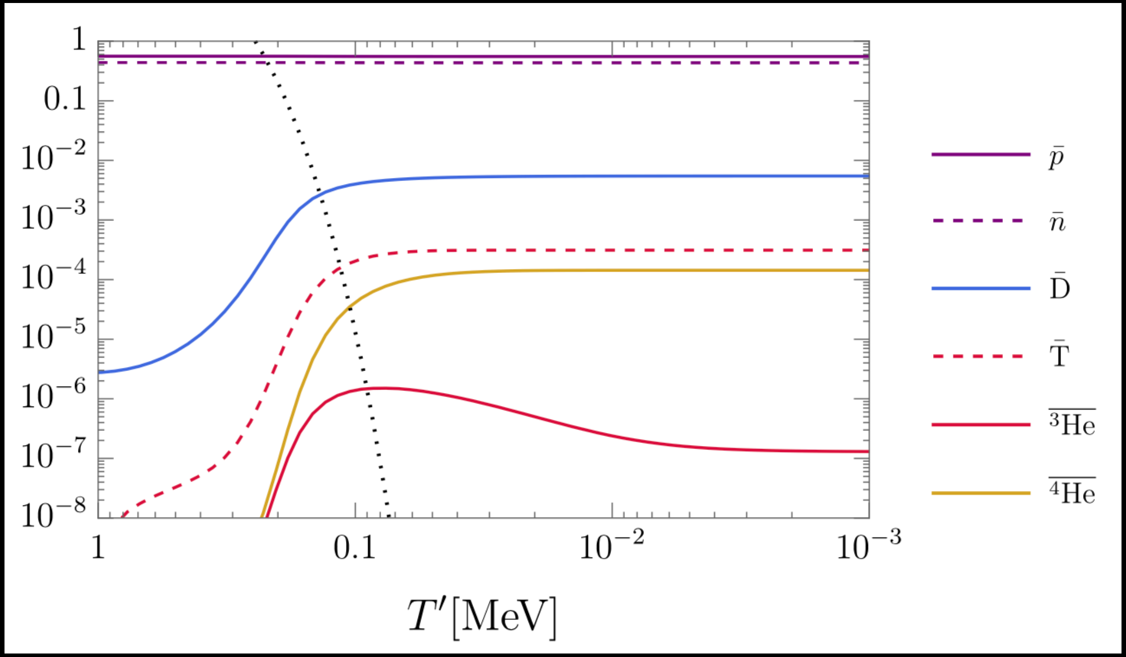

4) Antinucleosynthesis inside cosmic BSM fireballs

• The essential difference with BBN stems from the much larger rate with which the fireball temperature drops. The synthesis of elements heavier than antideuterium barely starts as the fireball rapidly expands, and is far from being complete when the plasma is released in interstellar space.

• The antideuterium abundance is approximately that generated by $\bar{n}$-$\bar{p}$ fusion reactions operating in a single dynamical expansion timescale at the point where antideuterium photodissociation freezes-out.

$$X_{\bar{\mathrm{D}}} \simeq n'_{\bar{B}} \, \langle \sigma v \rangle_{\bar{n}\bar{p}} \, \tau'_{\bar{\mathrm{D}}} X_{\bar{n}} X_{\bar{p}}$$

$$X_{\bar{\mathrm{T}}} \propto X_{\bar{\mathrm{D}}}^{3} \text{ while } X_{\overline{^4\mathrm{He}}} \propto X_{\bar{\mathrm{D}}}^{5}$$

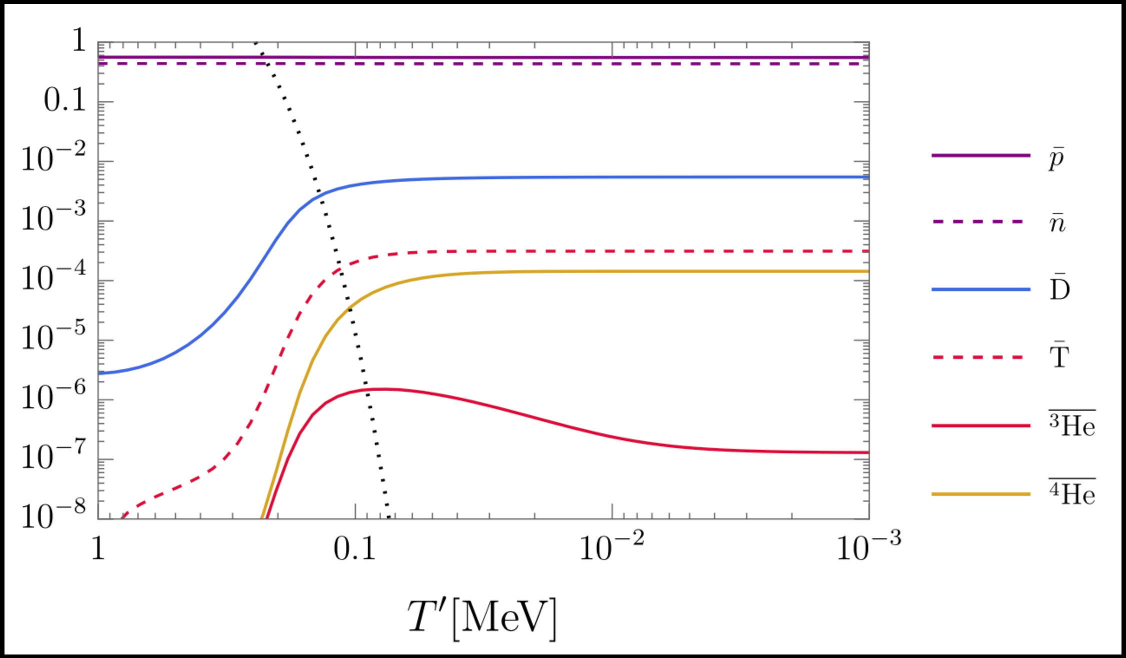

4) Antinucleosynthesis inside cosmic BSM fireballs

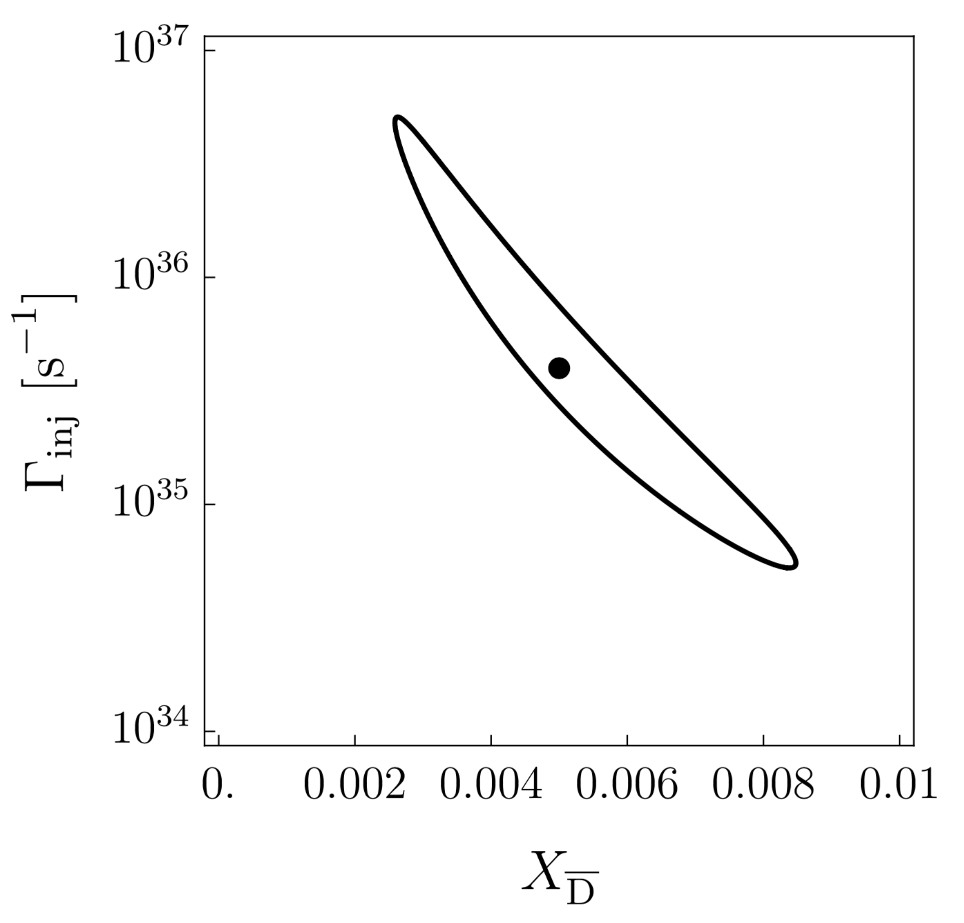

The region of parameter space for which AMS-02 would be expected to observe 3 events of $^4\overline{\rm He}$ and 6 events of $^3\overline{\rm He}$ in 10 years where $\Gamma_{\rm inj}$ is the injection rate of antinuclei in the Milky Way.

M. Fedderke et al., Phys. Rev. **D109** (2024) 123028

Takeaway

- $\overline{\mathrm{D}}$ events
  Antideuterium is expected to be detected in the cosmic radiation.
  Conventional processes yield a flux peaking at ~ 10 GeV.
  Events below ~ 1 GeV would point toward annihilating DM.

- $^3\overline{\mathrm{He}}$ events
  Unless CR propagation and coalescence are very different from expected,
  AMS-02 should **not** see secondary CR $^3\overline{\mathrm{He}}$.
  Interesting possibility from DM annihilating into $\bar{\Lambda}_b$ baryons.
  The branching ratio $\mathrm{Br}(\bar{\Lambda}_b \to \overline{^3\mathrm{He}})$ is a measurement of great importance.

- $^4\overline{\mathrm{He}}$ events
  There is no hope to detect a single event from CR spallation.
  A detection would require an exotic explanation.
  A QCD dark sector for instance, or BSM fireballs all over the Milky Way.

- Observation of $^3\overline{\mathrm{He}}$ and $^4\overline{\mathrm{He}}$ events would definitely be a major discovery, whose decipherment would require a precise measurement of the various CR antinuclei fluxes.

Thanks for your attention

Typical timescales for Galactic CR propagation

- From $\tau_{\rm inel} = (\sigma_{\rm ine}\, v_{\rm CR}\, n_{\rm ISM})^{-1}$, $\tau_{\rm diff} = hL/K$ and $\tau_{\rm conv} = h/V_C$, we build the typical timescale for the disk

$$\frac{1}{\tau_{\rm disk}} = \frac{1}{\tau_{\rm inel}} + \frac{1}{\tau_{\rm conv}\left\{1 - e^{-\tau_{\rm diff}/\tau_{\rm conv}}\right\}}$$

- Energy losses and diffusive reacceleration are respectively associated to the timescales $\tau_{\rm loss} = T/|b|$ and $\tau_{\rm DR} = T^2/D_{\rm EE}$.

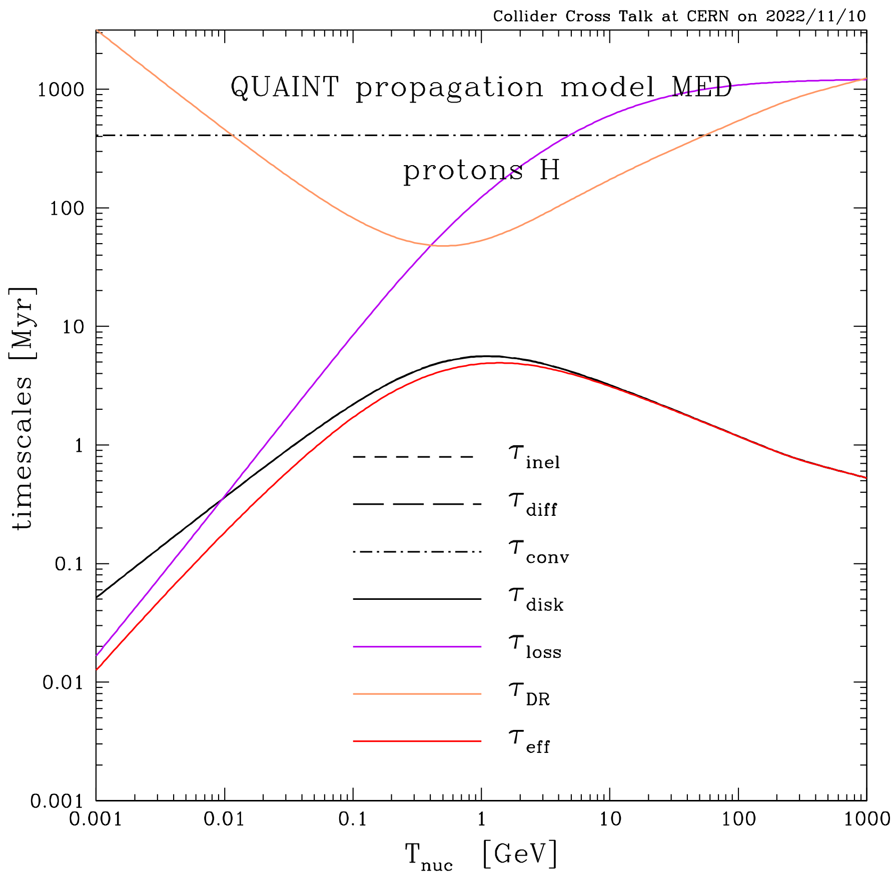

TABLE VI: Propagation parameters for the MIN, MED, and MAX configurations of the QUAINT models.

QUAINT	L [kpc]	δ	$\log_{10} K_0$ [kpc^2/Myr]	V_a [km/s]	V_c [km/s]	η
MAX	6.840	0.504	-1.092	83.929	0.469	-1.001
MED	4.080	0.451	-1.367	52.066	0.239	-2.156
MIN	2.630	0.403	-1.643	18.389	0.151	-3.412

Y. Génolini et al., Phys. Rev. **D104** (2021) 083005

Typical timescales for Galactic CR propagation

- From $\tau_{\rm inel} = (\sigma_{\rm ine}\, v_{\rm CR}\, n_{\rm ISM})^{-1}$, $\tau_{\rm diff} = hL/K$ and $\tau_{\rm conv} = h/V_C$, we build the typical timescale for the disk

$$\frac{1}{\tau_{\rm disk}} = \frac{1}{\tau_{\rm inel}} + \frac{1}{\tau_{\rm conv}\left\{1 - e^{-\tau_{\rm diff}/\tau_{\rm conv}}\right\}}$$

- Energy losses and diffusive reacceleration are respectively associated to the timescales $\tau_{\rm loss} = T/|b|$ and $\tau_{\rm DR} = T^2/D_{\rm EE}$.

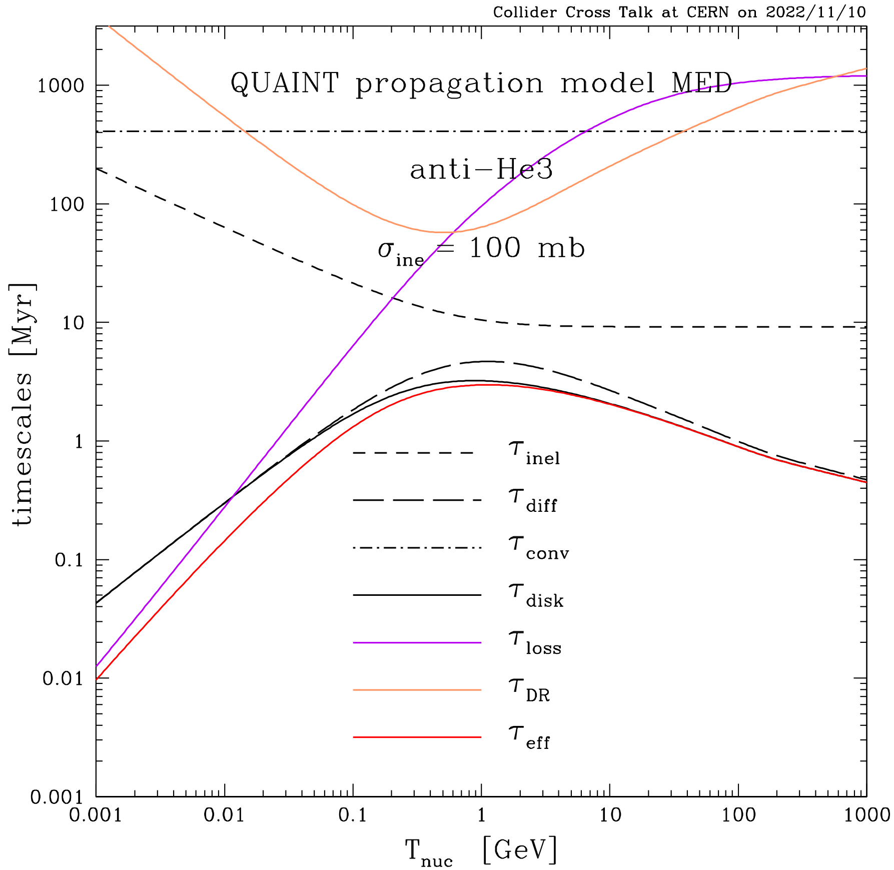

TABLE VI: Propagation parameters for the MIN, MED, and MAX configurations of the QUAINT models.

QUAINT	L [kpc]	δ	$\log_{10} K_0$ [kpc^2/Myr]	V_a [km/s]	V_c [km/s]	η
MAX	6.840	0.504	-1.092	83.929	0.469	-1.001
MED	4.080	0.451	-1.367	52.066	0.239	-2.156
MIN	2.630	0.403	-1.643	18.389	0.151	-3.412

Y. Génolini et al., Phys. Rev. **D104** (2021) 083005

Typical timescales for Galactic CR propagation

- From $\tau_{\rm inel} = (\sigma_{\rm ine} v_{\rm CR} n_{\rm ISM})^{-1}$, $\tau_{\rm diff} = hL/K$ and $\tau_{\rm conv} = h/V_C$, we build the typical timescale for the disk

$$\frac{1}{\tau_{\rm disk}} = \frac{1}{\tau_{\rm inel}} + \frac{1}{\tau_{\rm conv}\left\{1-e^{-\tau_{\rm diff}/\tau_{\rm conv}}\right\}}$$

- Energy losses and diffusive reacceleration are respectively associated to the timescales $\tau_{\rm loss} = T/|b|$ and $\tau_{\rm DR} = T^2/D_{\rm EE}$.

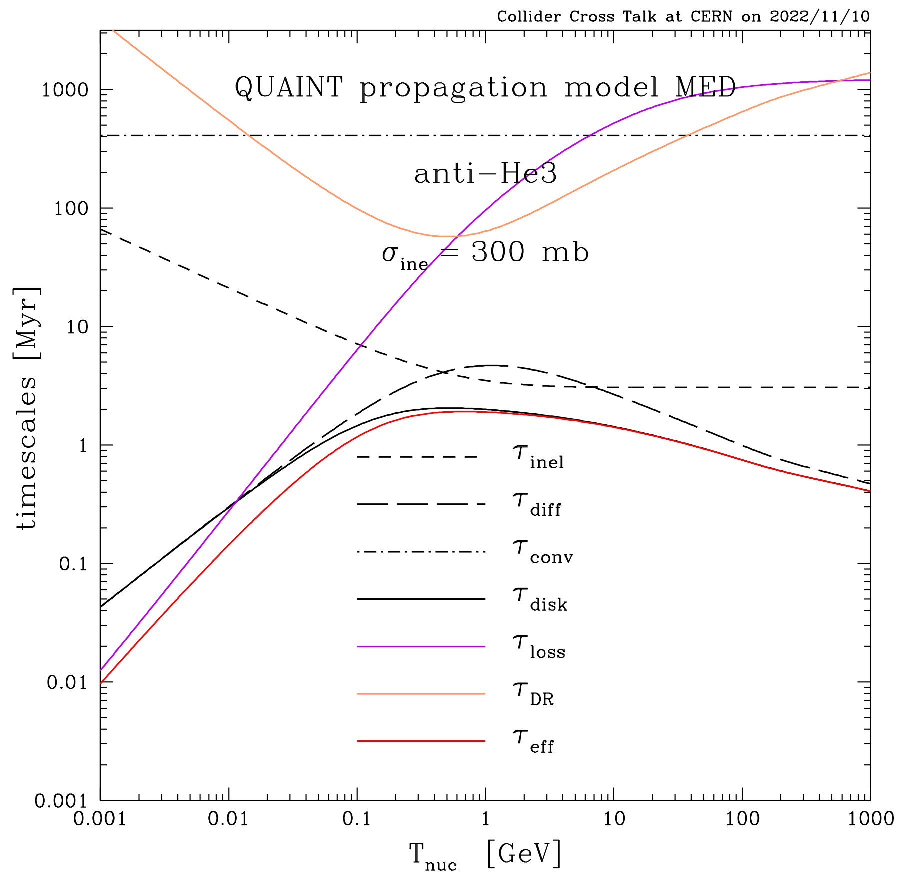

TABLE VI: Propagation parameters for the MIN, MED, and MAX configurations of the QUAINT models.

QUAINT	L [kpc]	δ	$\log_{10} K_0$ [kpc^2/Myr]	V_a [km/s]	V_c [km/s]	η
MAX	6.840	0.504	-1.092	83.929	0.469	-1.001
MED	4.080	0.451	-1.367	52.066	0.239	-2.156
MIN	2.630	0.403	-1.643	18.389	0.151	-3.412

Y. Génolini et al., Phys. Rev. **D104** (2021) 083005